Chemical Geology 528 (2019) 119285

Contents lists available at ScienceDirect

Chemical Geology

journal homepage: www.elsevier.com/locate/chemgeo

Invited research article

Environmental controls on mid-ocean ridge hydrothermal fluxes

Laurence A. Coogan[a,*], William E. Seyfried[b], Nicholas J. Pester[c]

[a] School of Earth and Ocean Sciences, University of Victoria, Victoria V8P 5C2, Canada
[b] Department of Earth Sciences, University of Minnesota, 310 Pillsbury Dr. SE, Minneapolis, MN 55455-0219, USA
[c] Department of Earth and Planetary Science, University of California, Berkeley, Berkeley, CA 94720, USA

ARTICLE INFO

Keywords:
Hydrothermal fluxes
Mid-ocean ridge
Seawater composition

ABSTRACT

High temperature hydrothermal fluxes at mid-ocean ridges are thought to be an important component of oceanic biogeochemical cycles. However, little consideration has been given to how these fluxes vary as a consequence of changing environmental conditions over Earth history. Here we consider how changes in sea level and ocean chemistry are likely to have impacted on-axis, high-temperature, hydrothermal fluxes focusing on Phanerozoic conditions. Changes in sea level lead to changes in hydrostatic pressure near the base of hydrothermal systems where both peak fluid-rock reaction temperatures and phase separation occur. In general, higher global sea level will lead to higher peak temperatures of fluid-rock reaction. Additionally, phase separation at higher pressure tends to lead to formation of a more Cl-rich vapor, that constitutes a larger mass fraction of the system. These combined factors may serve to significantly modify hydrothermal fluxes even for sea level changes on the scale of 100 m. Changes in ocean chemistry can also affect axial hydrothermal fluxes in several ways. Seawater sulfate contents control the amount of anhydrite that forms, which has both physical (porosity filling) and chemical effects. The most important aspect of ocean chemistry in controlling the composition of high-temperature vent fluids may be ocean salinity. If evaporite formation and dissolution has changed ocean salinity substantially over the Phanerozoic, hydrothermal fluxes could have been greatly modified. Ocean chemistry also plays a large role in controlling processes operating in hydrothermal plumes and hence the net flux of elements into and out of the ocean associated with hydrothermal systems. We conclude that there is a need for substantial further work to quantify the effects of sea level and ocean chemistry on high-temperature hydrothermal fluxes, including the development of more robust models that integrate field, laboratory and theoretical observations.

1. Introduction

Plate separation along the global mid-ocean ridge system leads to decompression mantle melting. The melt flows upward into the crust carrying a large heat flux, much of which is dissipated through advection of seawater-derived hydrothermal fluids at high-temperatures (~400 °C) near to the ridge axis. Reactions between the heated seawater and crust lead to significant chemical exchange followed by the return of chemically modified fluids to the ocean. While there is a continuum in the temperature (T) of hydrothermal fluids, and fluid flow occurs throughout the life of the oceanic crust, it is convenient to separate discussion of on- and off-axis hydrothermal systems. Here we discuss on-axis systems, which we define in this context as systems that are driven largely by magmatic heat (rather than lithospheric cooling), and hence we consider the hydrothermal systems along mid-ocean ridges.

Hydrothermal fluids carry chemical fluxes of importance for many global biogeochemical cycles. For example, hydrothermal fluxes have been suggested to be important in the major cation budgets of the ocean (e.g., de Villiers, 1998), in delivering micronutrients such as Fe and Zn to the deep ocean (e.g., Tagliabue et al., 2010; Roshan et al., 2016) and in moderating the isotopic composition of numerous seawater components (e.g., Li, O, Sr). However, the magnitudes of these chemical fluxes remain uncertain. Estimates of modern hydrothermal fluxes from mid-ocean ridges differ substantially with a significant part of the uncertainty resulting from how the axial flux is defined (e.g., Von Damm et al., 1985a; Elderfield and Schultz, 1996; Coogan and Dosso, 2012). A common approach to estimating the axial hydrothermal flux is to calculate the heat flux along the global ridge system, from this determine the mass flux of high-temperature hydrothermal fluid required to remove this heat, and then multiply this by the concentration of elements in high-temperature hydrothermal fluids. For example, the commonly used chemical flux estimates of Elderfield and Schultz (1996) assumes that all hydrothermal heat extraction out to 1 Myr off-axis is carried by

* Corresponding author.
E-mail address: lacoogan@uvic.ca (L.A. Coogan).

https://doi.org/10.1016/j.chemgeo.2019.119285
Received 30 April 2019; Received in revised form 10 August 2019; Accepted 23 August 2019
Available online 02 September 2019

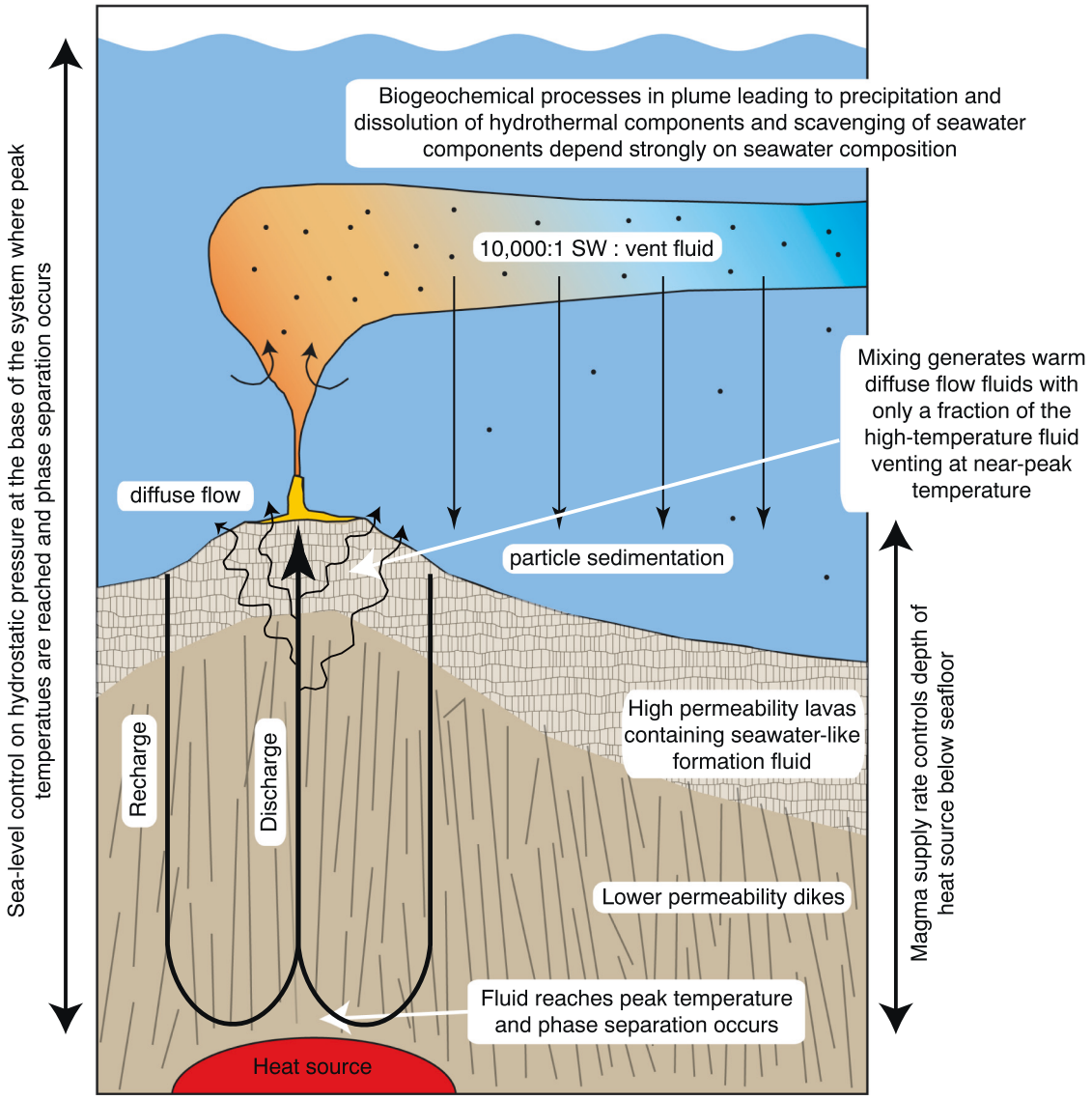

Fig. 1. Cartoon of a ridge axis hydrothermal system operating in the upper oceanic crust. Recharging seawater approaches a heat source near the base of the sheeted dike complex and becomes buoyant at temperatures similar to those of the liquid-vapor phase boundary. The hydrostatic pressure, which in part depends on sea level, is important to aspects of the physical and chemical evolution of the fluid. On crossing the dike-lava boundary the discharging fluid will tend to mix with the formation fluid in the lavas unless it gets focused into a high permeability channel (e.g., through anhydrite precipitation clogging the surrounding permeability). Mixing generates diffuse fluids, whereas channelized fluids vent at chimney structures and form plumes within the overlying water column. Within the hydrothermal plume particles form, and eventually settle out into sediment, but plumes can extend 1000's of km off-axis. For a modern-like system, with a flux of $\sim 1 \times 10^{13}$ kg yr^{-1} of high-temperature fluid, 10–50% of this vented at high temperature, and a 10,000:1 dilution factor in the plume the mass of the entire ocean will cycle through a plume every 30–140 kyr. The level at which the plume forms depends on the stratification within the ocean which may have varied over Earth history.

fluids with black-smoker like compositions. However, there is no evidence for high-temperature venting outside of a much younger axial zone. Indeed, such approaches can lead to unfeasibly large fluxes (e.g., the estimated hydrothermal fluxes of Li and K in Von Damm et al. (1985a) would remove > 100% of these elements from the entire ocean crust). Coogan and Dosso (2012) attempted to circumvent these problems using a combination of vent fluid and sheeted dike compositions and mass and isotope balance models. This approach provides an independent estimate of the fluid flux associated with fluid-rock reaction at temperatures appropriate to produce black smoker fluids and leads to smaller fluid and chemical fluxes. Both approaches use measured high-temperature vent fluid compositions as a key constraint on the global fluxes. However, an under-appreciated aspect of well-studied active black-smoker systems, with high heat output, is that these systems cannot be representative of steady-state condition at the ridge axis as their heat output exceeds the steady-state heat supply. Instead, regions of intense venting are in a state of high hydrothermal heat output that will diminish over time (e.g., Baker et al., 1996; Lowell et al., 2013; Gillis and Coogan, 2019). It is possible that chemical fluxes (and element/heat ratios) determined from these systems may be significantly biased relative to time integrated fluxes.

Approaches such as those described above produce a fixed estimate of the modern hydrothermal flux, however, when considering paleo-ocean chemistry the magnitude of paleo-hydrothermal fluxes need to be estimated. These are generally either assumed to remain constant (equivalent to modern), or to scale with estimates of paleo-oceanic crustal production rates (e.g., Berner et al., 1983; Demicco et al., 2005). However, there is no *a priori* reason that the crustal accretion rates should be the sole, or even dominant, control on mid-ocean ridge hydrothermal chemical fluxes over Earth history. Indeed, some authors have suggested that changes in environmental conditions can modify chemical fluxes. For example, Kasting et al. (2006) suggested that

changes in the average depth of mid-ocean ridges over Earth history affected hydrothermal fluxes of O-isotopes due to the role of pressure (P) in controlling the physical properties of hydrothermal fluids. Likewise, ocean chemistry has long been thought to play a fundamental role in the flux of Fe from the crust into the open ocean (e.g., Kump and Seyfried, 2005; Bekker et al., 2014). Here we consider such environmental controls on ridge-axis chemical fluxes in a more general context and focus on the Phanerozoic. We define an environmental control as being a change in bottom water temperature or composition and/or a change in the mean ocean depth above mid-ocean ridges (which, for brevity, we refer to as "sea level"). Variation in these parameters is linked to other changes in the Earth system such as atmospheric chemistry and climate. If changes in the broader Earth system lead to changes in on-axis chemical fluxes it will be important to incorporate these potential feedbacks into models of ancient ocean chemistry and Earth system evolution.

We start with a general introduction to oceanic hydrothermal systems, with a focus on those aspects where there is the greatest potential for environmental factors to affect hydrothermal fluxes (Section 2). We then address how axial hydrothermal fluxes are predicted to respond to changes in sea level and bottom water chemistry and temperature (Section 3). We address how both processes operating within the crust, and in the overlying water column, will affect axial hydrothermal fluxes. This is followed by two examples of how axial hydrothermal fluxes may have responded to changing environmental conditions over different intervals in the Phanerozoic (Section 4). We finish with some thoughts on future research directions required to better understand the links between on-axis hydrothermal fluxes and global environmental conditions.

2. Axial hydrothermal systems

Hydrothermal systems at mid-ocean ridges have been extensively studied since their discovery and numerous reviews provide extensive background on these systems (e.g., Seyfried, 1987; Von Damm, 1995; Alt, 1995; Lilley et al., 1995; Cann and Gillis, 2004; Tivey, 2007; German and Seyfried, 2014; Humphris and Klein, 2018). Only a brief summary of key features is provided here and we focus on those aspects that are likely to respond to changing environmental conditions.

Chemical exchange between the crust and ocean at mid-ocean ridges occurs across a wide range of temperatures and local water-to-rock ratios, leading to large spatial (and temporal) variations in chemical processes. The basic structure of the upper oceanic crust formed at intermediate- to fast-spreading ridges, and at some slow-spreading ridges, is a high permeability lava layer overlying a lower permeability dike complex (Fig. 1). Most fluid flow and fluid-rock reaction occurs in these basaltic composition layers which are underlain by a heat source (either a magma reservoir or solidified plutonic rocks). The plutonic rocks (largely gabbroic) that make up ~60–80% of the mass of the oceanic crust underlie the heat source and appear to be substantially less hydrothermally altered than the sheeted dikes although they have been studied far less due to their inaccessibility. The depth of the heat source below the seafloor increases with decreasing spreading rate from ~1 to 1.5 km at fast-spreading ridges to ≥3 km at slow-spreading ridges. Seawater is drawn down into the crust (in relatively cool recharge zones), precipitating anhydrite due to its retrograde solubility, and warms rapidly as it approaches the heat source. The fluid reaches peak temperatures, undergoes fluid-rock reaction and expands (and can phase separate; see below) and moves upwards. Fluid-rock reaction at the base of the system, and in the discharge zone in the sheeted dikes, typically occurs at ≥400 °C. Several lines of evidence suggest that time integrated water-to-rock ratios in black smoker systems are ~1 in the sheeted dike complex (Bickle and Teagle, 1992; Barker et al., 2008; Chan et al., 2002; Spivack and Edmond, 1987). As the upwelling high-temperature fluid crosses from the dikes into the overlying lavas the crustal porosity and permeability increase dramatically, and the majority of the fluid mixes with cooler (seawater-like) fluid in the lavas, becoming chemically modified prior to exiting the seafloor as so-called "diffuse flow" (Fig. 1). However, some fraction (~10–50%; Schultz et al., 1992; Chin et al., 1994; Ramondenc et al., 2006) of the high-temperature fluid that cross upwards from the dikes into the lavas is able to migrate through the lavas without substantial mixing, resulting in "black smokers" which commonly vent fluid at temperatures of 350–400 °C. Such high-temperature fluids can only reach the seafloor where there is an unusual permeability structure in the lavas that, at least in part, is due to sub-seafloor mineral precipitation that prevents mixing by isolating high-temperature upflow zones (e.g., Lowell et al., 2003). Seafloor chimney structures are built when mixing of high temperature fluids with seawater leads to mineral precipitation (e.g., Tivey, 2007). This mineral precipitation continues within the water column above hydrothermal vents where the high-temperature fluid is further diluted by seawater and buoyantly rises forming a hydrothermal plume (Fig. 1). Particles within the plume form by precipitation of hydrothermally sourced components, but seawater-derived components are also incorporated into particles during precipitation (co-precipitation) or can be scavenged from seawater later, leading to net negative fluxes of some elements. These particles largely settle out into seafloor sediments but can also dissolve as conditions change within the plume. The chemical fingerprint of hydrothermal input to the water column and seafloor sediments can be traced 1000's of km off-axis (e.g., Lupton and Craig, 1981).

2.1. Geodynamic boundary conditions

The primary geodynamic control on mid-ocean ridge hydrothermal fluid fluxes comes from the global rate of accretion of new oceanic crust. The rate of magma supply to the ridge directly controls the rate of hydrothermal heat extraction with all of the latent heat, and a significant fraction of the specific heat, removed within < 10 km of the ridge axis. On the modern Earth, at all but the slowest-spreading ridges, the extent of melting is almost independent of spreading rate, leading to near-constant crustal thickness (e.g., Reid and Jackson, 1981). Consistent with this is a linear increase in the incidence of hydrothermal plumes in the water column with increasing spreading rate (Baker et al., 1996). Thus, the global hydrothermal fluid flux is largely controlled by the global length of ridges and their mean spreading rate. At very slow spreading rates ($< 25\ mm\ yr^{-1}$) the crust is thinner, probably due to conductive heat loss to the surface, both decreasing the amount of melt produced and leading to significant crystallization within the mantle (e.g., Cannat, 1993). The heat flux available to drive hydrothermal flow is hence reduced relative to the rate of plate creation at very slow spreading ridges. Additionally, limited melt supply leads to the crust being a mixture of mantle peridotite and mafic rocks meaning that the primary mineralogy involved in fluid-rock interaction is more variable than at faster spreading ridges. However, on the modern Earth only ~10% of oceanic crust is formed at $< 25\ mm\ yr^{-1}$ and earlier in Earth history such magma-starved ridges were probably even less important.

The potential temperature of the upper mantle is the primary control on the thickness of oceanic crust (e.g., Klein and Langmuir, 1987) and hence the amount of heat available to drive hydrothermal circulation per area of new crust created. Earlier in Earth history, when the average upper mantle potential temperature was higher, fluid fluxes would thus probably have been larger for a given spreading rate. Additionally, in the same way that magma chambers at fast-spreading ridges are shallower than at slow-spreading ridges, higher magmatic heat fluxes into the crust earlier in Earth history would probably have led to shallower magma chamber depths to facilitate heat extraction. This would lead to fluid-rock reaction occurring at lower-pressure (if ocean depths where similar to modern values) and substantially higher water-to-rock ratio (due to the smaller mass of rock overlying the heat source). For example, doubling the crustal thickness (and hence doubling the heat available to drive fluid flow) and halving the thickness of

the sheeted dike complex would lead to a roughly four-fold increase in water-to-rock ratio within the sheeted dike complex. Higher mantle potential temperatures (by ~200 °C) early in Earth history (e.g., Herzberg et al., 2010) could have led to much shallower (and possibly even emergent) ridge axes with substantial implications for axial hydrothermal systems.

A final geodynamic control on the global average on-axis hydrothermal flux comes from the Wilson cycle (e.g., Müller et al., 2013). During a major continent rifting event (e.g., breakup of a super continent) the fraction of the global ridge network that is close to a continental margin will be large. Such ridges are likely to be sediment covered, which both changes the permeability structure of the crust and leads to chemical interaction between the sediments and hydrothermal fluid (Von Damm et al., 1985b; Lilley et al., 1993; Section 2.3.3). At non-volcanic rifted margins hydrothermal systems are likely to operate in ultramafic-rich lithologies, again impacting the bulk chemical fluxes associated with these systems. Additionally, both global sea level (e.g., Miller et al., 2005) and ocean salinity (Hay et al., 2006) are thought to be linked to the Wilson cycle and these both impact axial hydrothermal fluxes (see Section 3).

2.2. The physical and chemical properties of mid-ocean ridge hydrothermal fluids

The physical properties of seawater-derived hydrothermal fluids are dependent on the pressure and temperature conditions within the crust and hence are sensitive to changes in sea level. The chemical composition of both seawater and seawater-derived hydrothermal fluid is dominated by NaCl such that their phase relations and thermodynamic properties are similar to those of NaCl solutions (Bischoff and Rosenbauer, 1985; Bischoff, 1991). Substantial variability in the Cl-content of high-temperature vent fluids (Fig. 2), and correlated changes in other fluid species, suggest that phase separation is an import process in seafloor hydrothermal systems that plays a key role in the compositional variability of high temperature hydrothermal fluids at mid-ocean ridges (Butterfield et al., 1994; Coumou et al., 2009a, 2009b; Fontaine and Wilcock, 2007; McDermott et al., 2018; Pester et al., 2012; Seyfried et al., 2003; Von Damm, 1995; Von Damm et al., 2003). For any given temperature, phase separation can only occur at pressures below the critical pressure. The critical curve, defining the locus of critical P-T conditions, moves to increasing pressure and temperature with increasing fluid NaCl content in the system H_2O-NaCl (Fig. 3). The critical temperature and pressure of modern seawater (~3.2 wt% NaCl) is 29.8 MPa and 407 °C (relative to 22.1 MPa and 374 °C for pure water; Bischoff and Pitzer, 1989; Bischoff and Rosenbauer, 1985) which is broadly similar to the P-T conditions near the base of mid-ocean ridge hydrothermal systems. In a closed system at fixed P-T conditions, phase separation leads to coexistence of a vapor (V) and liquid (L) that have fixed compositions. However, small variations in temperature and/or pressure can result in substantial changes in their compositions (Fig. 3). In turn, this affects their physical (e.g., density, viscosity, enthalpy) and chemical properties and hence the chemical mass transport properties of hydrothermal systems (e.g., Driesner and Heinrich, 2007; Driesner, 2007). Importantly, the vapor is characterized by high enthalpy, and low viscosity and density, which are important from the standpoint of convective heat transport (Norton, 1984; Bischoff and Rosenbauer, 1985; Bischoff and Pitzer, 1989).

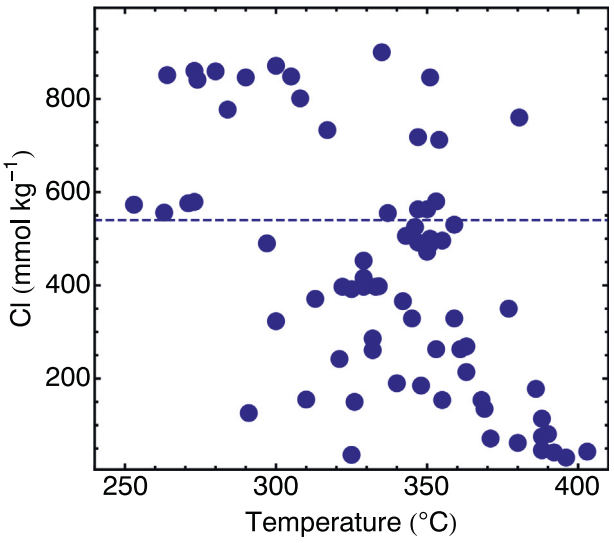

Fig. 2. Cross plot of vent fluid temperature and chlorinity for high-temperature vent fluids (> 250 °C) along the (fast-spreading) East Pacific Rise (data from ventDB). The large range of Cl demonstrates the importance of phase separation in MOR hydrothermal systems. While there is a lot of scatter, in general the higher temperature fluids have lower Cl contents than seawater (dashed line), and the lower temperature fluids higher Cl contents than seawater. The average vent fluid in this data compilation contains 416 ± 30 mmol kg^{-1} Cl substantially less than seawater.

Simulations of free convection of both pure water and NaCl solutions at elevated temperatures and pressures show that temperatures of upwelling plumes are effectively buffered by the physicochemical properties of fluid (e.g., Jupp and Schultz, 2004). Models show that pure water will tend to rise from a hot boundary layer at a temperature of ~400 °C irrespective of how much hotter than this the basal boundary is. This is due to a sharp increase in enthalpy, and decreases in viscosity and density, around this temperature that leads to conditions that maximize energy transport. This concept is described using the term “fluxability” which measures the ability of buoyancy driven fluid flow to transport heat (Jupp and Schultz, 2004; Lister, 1995). For seawater the maximum fluxability occurs around the onset of phase separation (i.e., near the two phase boundary) and is shifted to higher temperature with increasing pressure providing a fundamental link between the physico-chemical properties of hydrothermal fluids and ocean depth (Fig. 3d).

Although fluid-mineral reactions account for the major chemical differences between seawater and hydrothermal fluid (Section 2.3), phase separation leads to fractionation of dissolved components between the vapor and liquid phases. The behavior of dissolved species during phase separation can be described using experimentally derived partition coefficients, which can be calculated as a function of the ratio between either the density or salinity of the coexisting vapor and liquid phases (Bischoff and Rosenbauer, 1987; Berndt and Seyfried, 1997; Foustoukos and Seyfried, 2007; Pester et al., 2015; Pokrovski et al., 2005; Pokrovski et al., 2008). There is a strong correlation between salinity and density in these two-phase systems and, because the anion balance in deep-sea hydrothermal fluids is dominated by Cl^-, partitioning can be most simply calculated using the difference in chlorinity between the vapor and liquid (Fig. 4). Experiments show that the vapor is enriched in gaseous species such as H_2S and H_2 but is variably depleted in most metals (e.g., Li, Si, Ca, Mn, Fe, Zn, As, Rb, Sr, Cs) with the extent of depletion or enrichment dependent on the difference in Cl-content of the vapor and fluid (Bischoff and Rosenbauer, 1987; Foustoukos and Seyfried, 2007; Pester et al., 2015; Pokrovski et al., 2005). Under very lower pressure and high temperature condition the chemistry of hydrothermal vapors becomes exceptionally dilute (Von Damm, 2000; Seyfried et al., 2003), and partitioning behavior can change, leading to increases in Cl-normalized concentrations of many species in the vapor – a characteristic referred to as volatility (Foustoukos and Seyfried, 2007; Pester et al., 2015). Such conditions have been observed during and shortly after magmatic events, such as seafloor eruptions (Lilley et al., 2003; Pester et al., 2014) but may have been more widespread early in Earth history if ridges were much shallower.

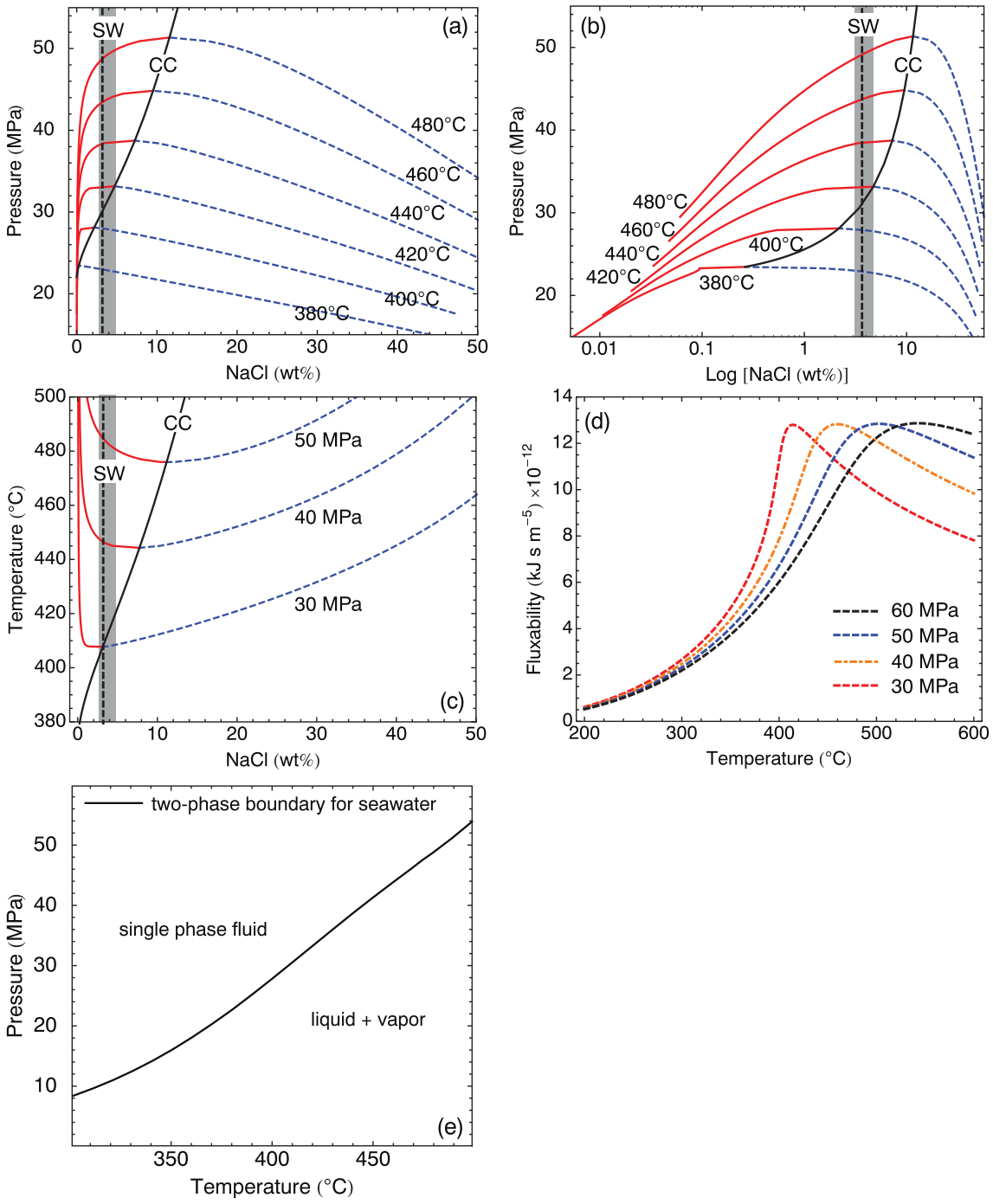

Fig. 3. Key physico-chemical properties of high-temperature aqueous fluids relevant to oceanic hydrothermal systems: (a & b) compositions of coexisting vapors (red, solid line) and liquids (blue dashed line) in the NaCl-H_2O system at different temperatures as a function of the pressure at which phase separation occurs shown on linear (a) and log (b) scale for fluid NaCl content; (c) compositions of coexisting vapors and liquids at different pressures as a function of the temperature at which phase separation occurs. In parts (a) to (c) the data are from Driesner and Heinrich (2007), the solid black line marks the critical curve (CC), the dashed vertical black line marks modern seawater NaCl content and the grey shading the likely range for the Phanerozoic seawater (SW; Hay et al., 2006); (d) fluxability (Eq. 8 of Jupp and Schultz, 2004) as a function of temperature for pure water with the fluid physical properties from the NIST steam tables (Lemmon et al., 2018). Note the shift in peak fluxability to higher temperatures with increasing pressure; (e) two-phase boundary between the liquid and liquid + vapor fields for modern seawater (3.2 wt% NaCl). This is the locus of the intersection of the dashed line marking seawater NaCl content and the two phase boundaries in parts (a) to (c) (Bischoff and Rosenbauer, 1988). See text for discussion.

2.3. *High-temperature fluid-rock reaction and fluid chemistry*

The composition of high-temperature vent fluids ("black smokers"), and comparison of these to fluids from experiments performed under conditions similar to those in the sheeted dike complex, provide important insights into hydrothermal fluxes. The low water-rock mass ratio (~1) in high-temperature mid-ocean ridge hydrothermal systems, and the high reactivity of the unaltered rocks at near peak hydrothermal temperatures, lead to the fluid composition being "rock-buffered" for many components; i.e., partial or complete equilibration between the fluid and mineral components lead to the chemical potential of most major dissolved species in the fluid either being fixed by,

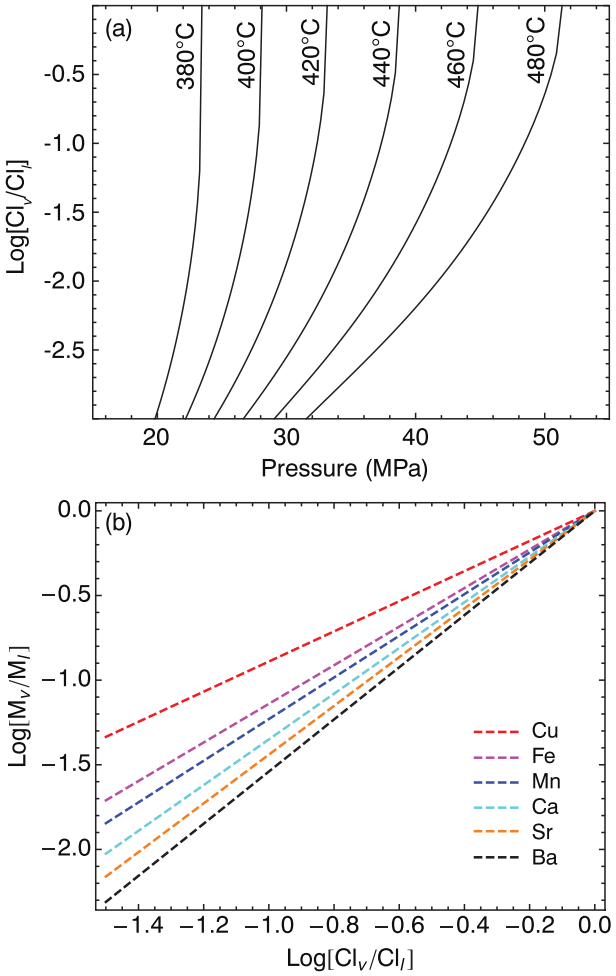

Fig. 4. (a) partitioning of Cl between vapor (v) and liquid (l) as a function of the P-T conditions of phase separation, and (b) how this controls the partitioning of elements (M) between vapor and liquid. Experimentally determined partitioning data from Table 2 of Pester et al. (2015). Phase separation under only slightly different P-T conditions generates vapors and liquids with substantially different Cl-contents which in turn leads to different partitioning of other elements between vapor and liquid. The positive slope for the metals shown reflects variable enrichment in the liquid phase, whereas species that become enriched in the vapor phase (mostly gases) exhibit a negative slope extending from the origin.

or at least driven towards, equilibrium with the mineral assemblage. However, the variability in the physico-chemical properties of the hydrothermal fluid (Section 2.2) lead to a wide range of high-temperature vent fluid compositions, with the concentration of many species in vent fluids correlated to the fluid Cl content.

2.3.1. Fluid-mafic rock interaction

Most fluid-rock reaction at mid-ocean ridges occurs between seawater-derived fluids and mafic rocks (largely basaltic dikes, but also gabbroic rocks and basaltic lavas). The igneous (plagioclase, clinopyroxene, ilmenite, magnetite, pyrrhotite ± olivine ± other accessory phases) and metamorphic (chlorite, amphibole, secondary plagioclase, quartz, epidotite ± pyrite ± talc ± titanite ± prehnite ± other accessory phases; e.g., Alt, 1995; Gillis et al., 2001; Alt et al., 2010; Heft et al., 2008) mineralogy of rocks altered at near peak fluid temperatures in the sheeted dike complex tightly constrain the activity of many aqueous components. Both experimental studies and the composition of high temperature vent fluids reveal almost complete removal of Mg and sulfate from seawater, and gains of Ca, Fe, K and Si. Anhydrite and (potentially) Mg-hydroxy-sulfate-hydrate (MHSH) precipitation lead to sulfate removal and also act as sinks for Ca and/or Mg (Bischoff and Dickson, 1975; Bischoff and Seyfried, 1978; Mottl and Holland, 1978; Mottl et al., 1979; Seyfried and Bischoff, 1981; Seyfried et al., 1991). These sulfate minerals are precipitated from seawater upon heating to ≥150 °C provided there is sufficient Ca (and Mg) in the seawater or leached from the rock. Sulfur concentrations and isotope ratios in vent fluids indicate that, at least in modern systems, only ~20% of seawater sulfate escapes precipitation into sulfates and is instead reduced to H_2S, prior to venting at the seafloor (Ono et al., 2007; Rouxel et al., 2008; Shanks, 2001; Barker et al., 2010; Alt et al., 1989). The existence of anhydrite places important constrains of the fluid redox conditions (Seyfried and Ding, 1995) that would not have existed when seawater sulfate levels were negligible (Kump and Seyfried, 2005). There is, however, little anhydrite in the rock record which may reflect its retrograde solubility and/or lack of sampling due to a heterogeneous distribution of this mineral (e.g., Alt et al., 2003). Equilibration with chlorite and/or amphibole at peak temperatures leads to a fluid with virtually zero Mg (Saccocia and Seyfried, 1994). At high-temperature (~400–450 °C) fluid-rock reactions involving secondary quartz, plagioclase, amphibole and epidote produce fluid Si and Ca contents generally consistent with those observed in black smokers (Berndt et al., 1988; Berndt and Seyfried, 1993; Scheuermann et al., 2018). At high temperature K (and the trace alkalis Li, Rb and Cs) is strongly leached from the rocks, with no mineral solubility limiting the fluid K content, leading to substantially elevated K contents of hydrothermal fluids relative to seawater. The activity of S-species, and heavy metals such as Fe and Cu, are generally buffered by oxide and sulfide minerals (e.g., pyrite, pyrrhotite, magnetite, chalcopyrite; Seyfried and Ding, 1995). Under these conditions the concentration of H_2S, H_2, Fe and Cu in the fluid are strongly dependent on the temperature, pressure, redox conditions, pH and the chloride content of the fluid (Ding and Seyfried, 1992; Seyfried and Ding, 1995). At very high temperatures Fe can become a major component. This is well demonstrated by the very deep vents from the Cayman trough (~5 km water depth) that have Fe > Ca, both of which can be explained by the very high peak fluid-rock reaction temperature (~500 °C; McDermott et al., 2018; Scheuermann et al., 2018). As discussed above, this high peak fluid temperature is expected due to the change in peak fluxability with changing pressure (Fig. 3). The net result of fluid-rock reaction is a hydrothermal fluid that is slightly acidic, reduced, and generally enriched in elements such as Li, Si, K, Ca, Mn, Fe and heavy metals, and depleted in Mg- and sulfate, relative to seawater.

2.3.2. Fluid-ultramafic rock interaction

Some portions of slow-spreading ridges have ultramafic lithologies mixed into the crust (Section 2.1). In such settings the mineralogy in the crust at peak hydrothermal conditions is different than in mafic systems, with peridotite (olivine, ortho- and clino-pyroxene and spinel) and serpentinite (serpentine, brucite, talc, tremolite, magnetite) mineral assemblages occurring, leading to somewhat different elemental behavior compared to systems hosted by solely mafic rocks (Allen and Seyfried et al., 2003; Bach and Klein, 2009; Charlou et al., 2002; Douville et al., 2002; Kelley et al., 2005; Seyfried et al., 2011; Wetzel and Shock, 2000). However, in nature a purely ultramafic source rock is unlikely to exist at shallow levels and instead hydrothermal fluids probably interact with a mixture of ultramafic and mafic rocks. This is supported by the composition of vent fluids from some "ultramafic hosted" systems (e.g., Rainbow on the MAR) that are highly reducing (e.g., high H_2 and CH_4), as expected for reaction with ultramafic rocks, but have lower pH, and higher Si and Fe contents, than predicted if the source was purely ultramafic (Douville et al., 2002; Seyfried et al., 2011). Although only a small fraction of the modern-day mid-ocean ridge hydrothermal flux is associated with ultramafic hosted systems these settings may have been more common during times of large-scale continental rifting because they are likely to be associated with non-volcanic rifted margins.

2.3.3. Sediment influenced ridges

When ridges are proximal to continental sediment sources, and sedimentation occurs rapidly during crustal accretion, seafloor eruptions are inhibited and shallow sill intrusion becomes a dominant mode of upper crustal accretion (e.g., Gieskes et al., 1982). Despite the low permeability sedimentary overburden, and mixed basalt-sediment uppermost crust, both focused high-temperature venting (and associated mineralization) and diffuse lower temperature venting still occurs in such setting (e.g., Guaymas Basin, Gulf of California; Middle Valley, Juan de Fuca ridge; Escanaba Trough, Gorda Ridge; Okinawa trough, South China sea; e.g., Lonsdale et al., 1980; Von Damm et al., 1985b; Fouquet et al., 1998). Fluid chemistry indicates phase separation occurs at sedimented ridges as it does at unsedimented ridges (James et al., 1999; Cruse and Seewald, 2006). However, there are systematic differences in some aspects of the chemistry of vent fluids at sediment hosted ridges compared to sediment starved ridges that can be explained by fluids reacting with sediments as well as basalts. These include higher alkalinity and higher B and alkali element concentrations, substantially lower transition metal concentrations, and the existence of ammonium as a major ion (e.g., Von Damm et al., 1985a, 1985b; Gieskes et al., 1982; James et al., 1999; Humphris and Klein, 2018). The low transition metal contents of venting fluids mean that plume processes will be different at sedimented ridges compared to unsedimented ridges. Perhaps the most striking difference in vent fluid chemistry at sedimented ridges is the much higher abundance of organic compounds that are, at least in part, derived from thermal alteration of organic matter in the sediments (Cruse and Seewald, 2006; Simoneit et al., 1992). These provide large carbon and energy sources for the biological communities associated with the hydrothermal vent (Martens, 1990; Teske et al., 2002). The flux of carbon in many different forms, the diversity of microbial metabolism, and the link between hydrothermal fluid circulation and the coexisting transport of petroleum, underscore the environmental uniqueness of these systems.

2.4. Mixing modifies net fluxes

High-temperature (~400 °C) hydrothermal fluids have their compositions largely set during fluid-rock reactions in rock-buffered systems within the sheeted dike complex. This makes the composition and temperature of seawater play a limited role in controlling the chemical evolution of the system. In contrast, when such high-temperature fluids mix with seawater the composition and temperature of seawater becomes much more important for the chemical evolution of the system. This is the case whether mixing occurs in the subsurface, leading to diffuse venting, or above the seafloor within hydrothermal plumes (Fig. 1).

2.4.1. Subsurface mixing

Although poorly constrained, multiple lines of evidence suggest that between ~50 and ~90% of the high-temperature hydrothermal fluid generated at depth in the crust mixes with a seawater-like formation fluid within the lavas, cooling to ≤50 °C before exiting the seafloor as diffuse flow (Schultz et al., 1992; Chin et al., 1994; Ramondenc et al., 2006; Coogan et al., 2017). During mixing species that are only stable in the high-temperature, reducing, hydrothermal end-member are precipitated, for example lowering the fluid H_2S and Fe contents (e.g., Butterfield et al., 1997; Foustoukos et al., 2009; Pester et al., 2008). The geological record of this mixing suggests that mineral precipitation is focused near the dike-lava boundary (Alt, 1995) although it can be seen throughout the lava pile. The chemistry of diffuse fluids entering the ocean are controlled by the compositions of the formation fluid and hydrothermal fluid, the relative proportion of each end-member (typically 1 to 10% high-temperature fluid), and reactions in the mixed fluid (in particular, mineral precipitation; Edmond et al., 1979; Schultz et al., 1992; Butterfield et al., 1997). The formation fluid may not match seawater exactly in either composition or temperature due to both low-temperature fluid-rock reactions in the lavas (e.g., Ravizza et al., 2001) and conductive heating by proximal black smoker fluids (e.g., Cooper et al., 2000). However, the composition of seawater is likely the dominant control on the composition of the formation fluid, and hence the composition of seawater may play an important role in the chemical evolution of diffuse fluids. The overall effect of subsurface mixing is to decrease the flux of relatively insoluble components into the ocean and increase their abundance in the lava section of the crust.

2.4.2. Plume processes

The portion of the high-temperature hydrothermal fluid that reaches the seafloor without substantial subsurface mixing (or conductive cooling) mixes into the ocean during and after venting. Mixing at, and immediately beneath, the seafloor leads to the formation of sulfide chimney structures (and ultimately massive sulfide deposits) characteristic of high-temperature venting. Mixing above the seafloor initially occurs within a buoyant plume at rapidly increasing seawater to vent fluid ratio until eventually the mixed fluid is no longer positively buoyant and it spreads laterally (Fig. 1). Over the first few seconds after exiting a chimney, very rapid mineral precipitation within the plume (generating the so-called “black smoke”) reflects the rapid changes in mixed fluid temperature, oxidation state and pH. Even within the first 20 m above the orifice of a black smoker vent a wide range of phases such as sulfides (e.g., pyrrhotite, pyrite, sphalerite and chalcopyrite), sulfates (anhydrite and barite), amorphous silica, Fe-oxyhydroxides and organic matter have been identified (Mottl and McConachy, 1990). The ratio of Fe to H_2S in the vent fluid plays a key role in the chemical evolution of the plume. If vent fluids have Fe < H_2S, much of the Fe is precipitated rapidly into sulfide minerals, whereas, if Fe > H_2S then significant amounts of Fe is precipitated more slowly via oxidation forming Fe-oxyhydroxides (e.g., Baker and Massoth, 1987; Mottl and McConachy, 1990). This is important because the relative abundance of Fe-sulfides and Fe-oxy-hydroxides controls the fate of many other elements as well as affecting the long-range dispersal of Fe in the open ocean.

Elements can be removed from seawater by co-precipitation with, and scavenging on to, hydrothermal particles. Oxyanions (e.g., P, V, As and Cr) are co-precipitated with Fe-oxyhydroxides (e.g., Feely et al., 1990, 1992) and this may, at least at times, have been a significant sink for the limiting nutrient P. The relative rates of plume dilution (supplying oxyanions from seawater) and Fe-oxyhydroxide precipitation in the buoyant plume, along with competition between oxyanions for incorporation, are thought to control the oxyanion/Fe ratio in Fe-oxyhydroxide particles (Rudnicki and Elderfield, 1993; Metz and Trefry, 1993). The rate of Fe-oxyhydroxide precipitation depends on seawater pH, O_2, temperature and salinity (Millero et al., 1987) all of which have changed substantially over Earth history. Other elements are co-precipitated into the sulfates anhydrite and barite, that form rapidly in the buoyant plume, stripping them from seawater (e.g., REE's; Chavagnac et al., 2018).

Within the non-buoyant plume some elements are scavenged from seawater onto Fe-oxyhydroxides (e.g., Th, REEs) and some further enrichment in oxyanions may occur (e.g., Ruhlin and Owen, 1986; German et al., 1990; Pavia et al., 2018; Ho et al., 2018). Oxidative dissolution of sulfide particles that are sufficiently small not to have settled out close to the ridge axis releases further Fe into solution, subsequently generating more Fe-oxyhydroxide particles. For example, ~10% of Fe in high-temperature vent fluids has been suggested to be in the form of nano-particle pyrite with settling times of ~1000 years (Yücel et al., 2011), and dissolution timescales of months to years, allowing its widespread dispersal (Gartman and Luther, 2014). Large scale transport of both hydrothermal (e.g., Fe, Mn) and seawater-derived (e.g., oxyanions, REEs) components has long been known from the compositions of seafloor sediments that are enriched in Fe and Mn many 100 s of km from ridges (Boström et al., 1969; Dymond et al., 1977). Consistent with this, recent work has confirmed that

hydrothermal plumes are enriched in dissolved and particulate Fe, Mn and Zn for 1000s of km away from ridges (Resing et al., 2015; Roshan et al., 2016; Fitzsimmons et al., 2017) with dissolved Fe probably stabilized in part by organic ligands (e.g., Gledhill and van den Berg, 1994).

Both the topography at the ridge axis and the stratification of the overlying water column affect the dispersal of hydrothermal plumes. Slow-spreading ridges generally have deep axial valleys that can both partially capture hydrothermal plumes, limiting their spread off-axis, as well as constraining the flow of bottom water currents that transport plumes. In contrast, the axial highs associated with intermediate- to fast-spreading ridges allow plumes to escape off-axis more readily. Water column stratification can also affect plume dispersal. For example, in the Artic the weakly stratified water column allows hydrothermal plumes to spread over an anomalously wide region (Baker et al., 2004).

3. Response of axial hydrothermal systems to changing environmental conditions

In this section we discuss, at a conceptual level, the effects of environmental changes on axial hydrothermal fluxes due to (i) changes in sea level (Section 3.1); (ii) changes in ocean chemistry that influence fluid-rock reactions (Section 3.2); and (iii) changes in ocean chemistry and temperature that modify mixing processes (Section 3.3). The discussion is focused on the kinds of environmental changes expected over the Phanerozoic – larger changes may be expected going further back in Earth history.

3.1. Sea level and the role of hydrostatic pressure on hydrothermal fluxes

The mean depth of the ocean has varied over Earth history for reasons such as the growth of continental ice-sheets, variations in the water content of the hydrosphere and changing hypsography. Ocean depth directly affects the hydrostatic pressure in the crust where high-temperature fluid-rock reactions occur, and this has been hypothesized to have affected hydrothermal fluxes over Earth history (Kump and Seyfried, 2005; Kasting et al., 2006). For example, currently a typical fast-spreading ridge axis has a seafloor depth of ~2500 m, and an underlying magma chamber ~1500 m below the seafloor. This yields a combined hydrostatic load of 4000 m near the roof of the magma chamber, which translates to a maximum reaction pressure of ~40 MPa. Changes in sea level of 100 to 500 m would therefore change this pressure by 2.5 to 12.5%, changes which have substantial effects on the physico-chemical properties of seawater (Figs. 3 & 4). Because the depth of the magma chamber (and seafloor) generally increases with decreasing spreading rate, the relative change in pressure at the base of the hydrothermal system for a given change in sea level is greater for faster spreading ridges. In this section we investigate how changes in ocean depth may impact net hydrothermal fluxes through the pressure dependence of: (i) the hydrothermal fluid temperature at peak fluxability; and (ii) the compositions and mass fractions of liquid and vapor produced by phase separation. While these topics are intimately related they are discussed separately for clarity.

3.1.1. The effect of sea level on hydrothermal fluxes due to changing peak fluid temperature

The temperature at which hydrothermal systems operate most efficiently to transport heat (i.e., maximum fluxability) is a function of hydrostatic pressure (Fig. 3d) due to the effect of pressure on the physical properties of the fluid (Lister, 1995; Jupp and Schultz, 2004; Fontaine and Wilcock, 2006; Coumou et al., 2008). At the same time, element solubility is strongly temperature dependent. Thus, the change in fluid temperature at peak fluxability will directly affect the capacity of the fluid to transport dissolved ions and hence sea level changes will propagate into changes in the hydrothermal metal flux (e.g., Pester,

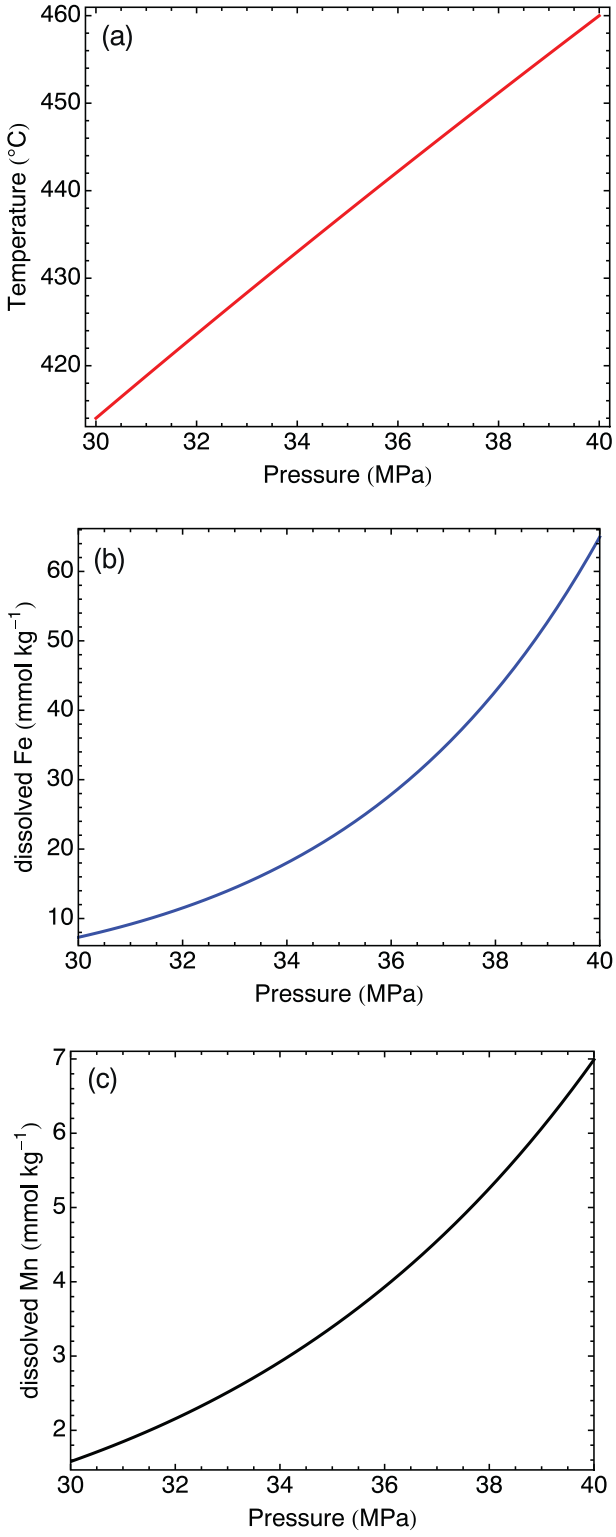

Fig. 5. The effect of pressure at the base of the hydrothermal system on the hydrothermal fluid temperature and composition: (a) change in upwelling fluid temperature (i.e., fluid temperature at peak fluxability) as a function of pressure for pure water (data from Lemmon et al., 2018); (b) change in fluid Fe content as a function of changing pressure across a pressure range equivalent to 1000 m change in sea level driven solely by the change in temperature from part (a); (c) as part (b) but for Mn. Changes in fluid Fe and Mn content are determined from log-linear regression through fluid compositions determined in basalt-seawater experiments at various temperatures (Pester et al., 2011; Fe = $10^{-7.68+0.0206T}$; Mn = $10^{-5.61+0.014T}$; with T in Celsius and concentrations in mmol kg^{-1}).

2018). As an example, we consider changes in the Fe and Mn content of hydrothermal fluids with changes in hydrostatic pressure because the temperature dependence of the solubility of these elements in hydrothermal fluids in equilibrium with basalt is relatively well constrained (e.g., Fig. 1 of Pester et al., 2011). Between 30 and 50 MPa (3 to 5 km of hydrostatic load), changes in the temperature at peak fluxability are weakly non-linear, with a pressure dependence of the temperature at peak fluxability of ~4.4 °C MPa^{-1} (Fig. 5a). This temperature change translates into increases in the concentration of Fe and Mn of 20–25% and ~15%, respectively for a 1 MPa increase in hydrostatic pressure (Fig. 5). While the empirical approach used here is unlikely to be accurate in detail, this simple model indicates that even a 100 m change in sea level could measurably effect metal mobilization from the crust. However, the metal content of hydrothermal fluids can be substantially modified prior to venting into the ocean (Section 2.4), and caution is required in directly extrapolating these values into hydrothermal fluxes into the ocean.

3.1.2. The effect of sea level on hydrothermal fluxes due to phase separation

Phase separation commonly occurs in oceanic hydrothermal systems generating a wide range of fluid Cl-contents (Fig. 2). The compositions, and hence mass fractions, of the vapor and liquid produced depend on the pressure and temperature at which phase separation occurs (Fig. 3). This means that changes in sea level will lead to changes in the composition and mass fraction of the vapor and liquid in on-axis hydrothermal systems. Because the vapor is less dense and less viscous than the liquid (e.g., Driesner, 2007; Palliser and McKibbin, 1998) it is thought to be more readily vented from the crust. This hypothesis is consistent with the observation that the highest temperature vent fluids generally have Cl contents somewhat lower than seawater and also with the observation that black smoker fluids, on average, have Cl-contents lower than that of seawater (Fig. 2). However, it should be noted that this observation is based on point sampling of fluids, and if the flux out of high Cl vents is higher than that from low Cl vents the flux averaged vent fluid Cl content may match that of seawater. The Cl-rich liquids have been suggested to either form a dense basal layer (e.g., Bischoff and Rosenbauer, 1989) or fill stagnant voids (e.g., Fontaine and Wilcock, 2006). In either model the higher salinity fluid is trapped in the crust until the system cools and mixing allows the liquid to be diluted and escape the crust (Schoofs and Hansen, 2000; Coumou et al., 2009a, 2009b). The lower temperature of the liquid phase when it vents from the crust will reduce its capacity to transport those species that have temperature-dependent solubility relative to if it had been lost from the crust with the vapor at peak temperature. This leads us to consider whether changes in sea level could, through changes in the pressure at which phase separation occurs, lead to variations in hydrothermal fluxes.

To semi-quantitatively illustrate the role that the pressure at which phase separation occurs could have on net hydrothermal fluxes we consider the following simplified model. Fluid is heated until it reaches the two phase boundary and oversteps this boundary by a small amount driving phase separation. The fluid is assumed to have a fixed composition before phase separation occurs and elements are partitioned between the vapor and liquid during phase separation based on experimentally derived partition coefficients (Fig. 4) and mass balance constraints. The vapor is then assumed to vent from the crust with no further chemical modification and the liquid remains in the crust until the system has cooled and mixing dilutes it allowing it to escape from the crust. As an end-member model we assume that non-conservative species partitioned into the liquid during phase separation are completely redeposited (due to cooling and dilution) in the crust prior to the fluid being vented. As the pressure (and hence temperature) at which phase separation occurs increases, the vapor becomes more Cl-rich increasing its capacity to transport most species (Figs. 3, 4 & 6). Additionally, with increasing pressure (and temperature) the mass fraction of vapor increases relative to that of liquid (because the increased Cl in the liquid means less can form by mass balance; Fig. 6). Experimental data on the partitioning of species between coexisting vapors and liquids allow these effects on the hydrothermal flux to be quantified (Fig. 4).

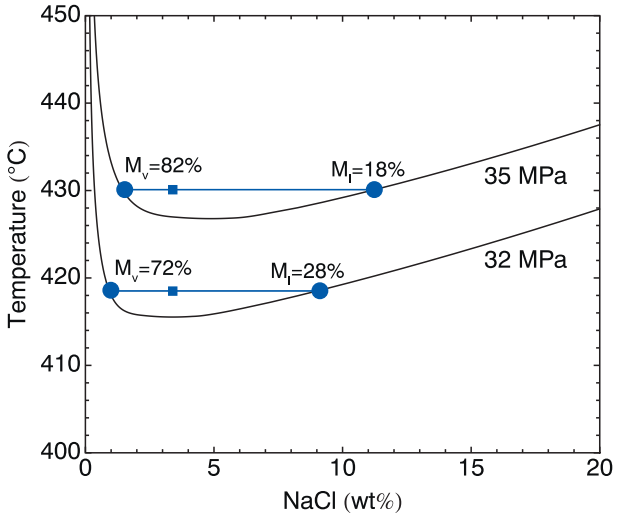

Fig. 6. Phase relations in the H_2O-NaCl system plotted for 32 MPa and 35 MPa (black lines). Also shown are the positions of the coexisting vapor and liquid produced at these pressures by heating modern seawater to 3 °C above the two phase boundary (blue circles connected by a line; modern seawater NaCl at these temperatures are shown by small squares). The mass fraction of the initial fluid that is partitioned into the vapor (M_v) and liquid (M_l) are also shown. Phase separation at higher pressure leads to a larger fraction of vapor with a higher salinity. Venting of such vapors, and retention of the liquids in the crust, would lead to an increase in the flux of those elements that partition into the liquid with increasing pressure. See text for discussion.

As an example of the process just described we consider the behavior of Fe using the partitioning data of Pester et al. (2015). We consider phase separation occurring at 32 and 35 MPa and assume a 3 °C overstep of the two-phase boundary (although the exact overstep makes little difference to this result). Under these assumptions the total Fe content of the vapor increases ~70% with this 3 MPa increase in the pressure at which phase separation occurs. This increase in the efficiency of Fe removal from the crust is due to the additive effects of the higher Cl content of the vapor at higher pressure (which increases the partitioning of Fe into the vapor relative to the liquid) and the smaller mass fraction of liquid at higher pressure leading, via mass balance, to a larger fraction of the Fe being in the vapor. The effect of pressure on fluid temperature (Section 3.1) is ignored in this calculation, although in nature it would further enhance the increased Fe flux. This example illustrates that relatively small increases in the mean hydrostatic pressure along the mid-ocean ridge system could lead to considerable changes in the extent of extraction of metals from the crust solely through the effect of pressure on phase separation and hence on the physical and chemical transport properties of these system. The flux of elements that partition into the vapor (e.g., H_2S) may be slightly decreased as the pressure at which phase separation occurs increases. Importantly, this means that an increase in hydrostatic pressure should lead to an increase in the average Fe/H_2S of vent fluids. These calculations are obviously very simplistic, and are presented only to illustrate that non-trivial changes in the average vent fluid composition could occur due to changes in average hydrostatic pressure at which phase separation occurs.

In summary, while the examples given in this section are only meant to be illustrative of potential effects, it seems likely that increased hydrostatic pressure associated with higher sea level will increase the efficiency of removal of many metals from the crust at high temperatures. This is due to both an increase in peak hydrothermal fluid

temperature (Section 3.1.1) and due to the increased salinity and mass fraction of the vapor produced during phase separation. These effects appear to be of similar magnitude although there are large uncertainties. Neither the details of the porosity and permeability structure of the crust, nor the role of subsurface mixing and mineral precipitation during discharge are known sufficiently well to allow accurate models of this system irrespective of how sophisticated the modeling approach used. Furthermore, the calculations presented above are inherently simplistic in that the fluid composition is assumed to be set at the base of the system but alteration of the oceanic crust demonstrates that fluid-rock reaction continues during discharge (Heft et al., 2008; Coogan, 2008; Alt et al., 2010). Thus, testing whether natural systems behave in the manner suggested here will probably require evidence from field observations.

3.2. Ocean chemistry and its role in high-temperature fluid-rock reaction

Ocean chemistry has changed over Earth history and hydrothermal fluxes are both dependent on these changes and a factor in driving them. Variations in trace element and isotope mass balances depend on ocean chemistry and have been widely discussed – we do not consider these in detail here. Instead we focus on the role of ocean chemistry in the phase equilibria that control hydrothermal fluid compositions due to changes in ocean NaCl content (referred to as salinity) and the abundance of other major ions (principally Mg, Ca and sulfate).

3.2.1. The effect of ocean salinity

Seawater salinity is thought to have changed over Earth history both due to changes in the mass of H_2O in the ocean basins (e.g., due to ice sheet formation) and due to changes in fluxes of Cl and associated cations into and out of the ocean (largely associated with evaporite deposition and weathering). Hay et al. (2006) suggest that seawater salinity has varied substantially over the Phanerozoic, ranging from ~35‰ to 45–50‰, and Neoproterozoic glaciations may have been associated with still higher salinities. This large range of salinity will have changed the behavior of hydrothermal systems during phase separation, for example, increasing the critical pressure and temperature with increasing ocean salinity. Also, because Cl is by far the dominant anion, and is largely conservative during fluid-mineral exchange, the concentration of most species correlates strongly with Cl in high-temperature hydrothermal fluids. Thus, an increase in seawater salinity is expected to increase the hydrothermal flux of many elements (e.g., Seyfried et al., 2002). For example, because plagioclase and quartz are part of the reacting assemblage at peak temperatures in almost all basalt-hosted mid-ocean ridge hydrothermal systems the (simplified) equilibria (aq: aqueous):

$$CaAl_2Si_2O_8 + 4SiO_2 + 2NaCl^{aq} = 2NaAlSi_3O_8 + CaCl_2{}^{aq} \quad (1)$$

is expected (Berndt and Seyfried, 1993; Seyfried et al., 2002; Pester et al., 2012). Assuming activity coefficients are approximately constant, Eq. (1) indicates that hydrothermal vent fluid Ca contents should increase as the square of the hydrothermal fluid salinity (Fig. 7) as observed experimentally (Berndt and Seyfried, 1993; Seyfried et al., 2002; Pester et al., 2012).

The process of phase separation complicates quantifying the simple scenario of increasing hydrothermal Ca flux with increasing seawater salinity described by Eq. (1). Assuming a fixed P-T structure within a hydrothermal circulation cell, the P-T condition at which phase separation occurs will change depending on the initial salinity of seawater. In turn, this means that the compositions of the vapor and liquid will also depend on the initial seawater composition. For example, at 40 MPa, increasing seawater salinity will decrease the temperature at which phase separation occurs, producing a more Cl-rich vapor and less Cl-rich liquid (cf. Fig. 3c). Conversely, if phase separation were to occur at a fixed P and T, a change in seawater salinity would simply change the relative mass fractions of liquid and vapor (not their compositions).

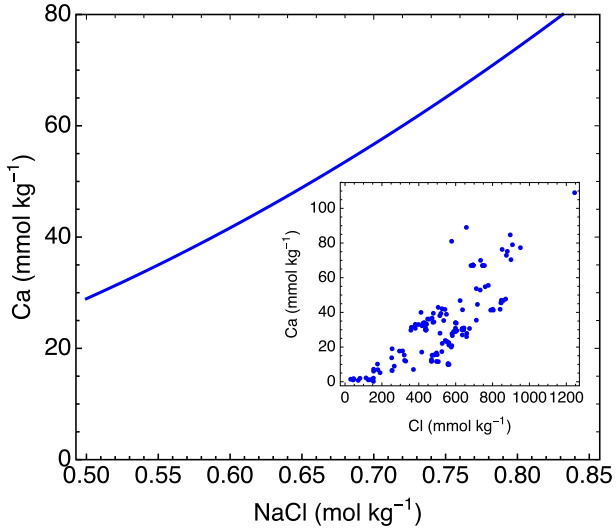

Fig. 7. Predicted increase in average hydrothermal vent fluid Ca content with increasing seawater salinity. This is calculated based on equilibrium between quartz, a fixed composition plagioclase and a NaCl-H_2O fluid (Eq. (1)). In this system $a_{CaCl_2} \propto a_{NaCl}{}^2$ and for illustrative purposes we have assumed activity coefficients of unity and fit a curve through a modern typical vent fluid Ca content of 35 mmol kg^{-1} at seawater salinity. While only a rough approximation of the true system, this calculation shows changes in seawater salinity of the scale expected over the Phanerozoic could have significantly impacted hydrothermal fluxes. The inset shows the correlation between Ca and Cl in modern vent fluids (T > 250 °C; from ventDB).

Thus, while Eq. (1) provides a simple way to approximate the effects of seawater salinity on hydrothermal Ca fluxes an accurate model will require quantification of the chemical and physical effects of phase separation.

3.2.2. The effect of seawater major ion composition

In addition to changes in bulk salinity, fluctuations in the relative abundance of the other major components in seawater (Mg, Ca, K and sulfate) have occurred throughout Earth history (e.g., Lowenstein et al., 2014). It is important to note that the composition of Phanerozoic seawater is imperfectly constrained. Of particular relevance to oceanic hydrothermal system is that constraints on the Ca and sulfate contents of paleoseawater from fluid inclusions in halite are not independent; instead, precipitation of gypsum, anhydrite and calcite prior to fluid inclusion trapping depletes the fluid in either Ca or sulfate, whichever is lower in concentration in the primary seawater. Thus, the minimum concentration for one or other element can be determined and estimates of the range of plausible concentrations for both are made by assuming their concentration product has remained within a narrow range over the Phanerozoic (e.g., Lowenstein et al., 2014). This is important in terms of the behavior of anhydrite in axial hydrothermal systems. The assumed fixed Ca and sulfate concentration product is equivalent to assuming the recharge fluid at mid-ocean ridges has a fixed anhydrite saturation state. Other assumptions are required to estimate the concentrations of other elements (e.g., Lowenstein et al., 2014). However, there clearly have been substantial variations in Phanerozoic seawater composition, including times of Ca > sulfate, and we consider how these may have affected high-temperature hydrothermal fluxes.

The role of changes in seawater chemistry in controlling high-temperature hydrothermal processes are currently not well constrained. Considering the low water-to-rock ratio in axial hydrothermal systems, fluid chemistry at high-temperatures is expected to be largely “rock buffered”. However, the evolution of the hydrothermal fluid chemistry is at least partially dependent on the starting fluid composition. It has long been known from experimental studies that reacting basalt with simple NaCl solutions of seawater salinity yields less exchange, and

produces a different fluid composition, than if the starting fluid is natural seawater (Seyfried and Bischoff, 1981). Within the recharge zone, where temperatures are relatively low and water-to-rock ratios high, precipitation of minerals such as anhydrite are expected be impacted by the composition of seawater. Currently, with Ca < sulfate in seawater, after all Ca is precipitated into anhydrite sulfate remains and can drive anhydrite precipitation deeper in the system using Ca leached from the crust. At times with seawater sulfate < Ca, sulfate may not have penetrated as deeply into the crust. Given the important role for anhydrite in fixing the redox state of high-temperature vent fluids (e.g. Seyfried and Ding, 1995) then this may have impacted hydrothermal fluxes. However, such effects are more likely to have been important during those parts of the Precambrian when sulfate levels were negligible (Kump and Seyfried, 2005).

Recently Antonelli et al. (2017) developed a model that explores the role of changing seawater Mg, Ca and sulfate over the Phanerozoic in changing the hydrothermal flux of these elements and Sr (c.f. Turchyn et al., 2013). For the major ions they used reaction path models to show that at low-temperatures (250–300 °C) and/or high water-to-rock (> 5) ratios the starting fluid composition is important in controlling the hydrothermal fluid composition; however, this effect diminishes substantially with increasing temperature and decreasing water-to-rock ratio (their Fig. S1). They then used a simplified model, based on a charge balance approach, to investigate possible effects of changing seawater composition on hydrothermal Ca and Sr fluxes over the Phanerozoic. In their model, loss of all of the Mg and sulfate from seawater is charge balanced by leaching Ca from the rock, accounting for anhydrite precipitation during the process. In nature some of this charge balance is accommodated by changes in other ions. For example, at high-temperatures Ca is lost from the fluid in exchange for Fe with some vent fluids generated at very high-temperatures (> 500 °C) having Fe > Ca on a molar basis (e.g., McDermott et al., 2018). Likewise, the large amounts of K leached from the crust must play a role in charge balance. Also, because the method of estimating paleoseawater compositions from fluid inclusions assumes the concentration product of Ca and sulfate is constant, changes in either of these automatically creates a charge imbalance in the estimated seawater composition. For example, the difference in charge between Mg and sulfate in seawater, that must be charge balanced by leaching ions from the crust in the model of Antonelli et al. (2017), is 50 equivalents kg^{-1} for modern seawater and 40 equivalents kg^{-1} for the Cretaceous. Whether this is real, and if so how charge balance was maintained in the Cretaceous, may be important for the veracity of the results of the Antonelli et al. (2017) model.

However, despite the caveats just discussed, the Antonelli et al. (2017) model provides a starting point for considering changes in hydrothermal fluxes due to changes in seawater Mg, Ca and sulfate contents. Using this approach, Antonelli et al. (2017) suggest that average modern axial hydrothermal systems contain ~5 mmol kg^{-1} (25%) more rock derived Ca than Cretaceous ones (data from their Fig. 2). In their model, they assume that anhydrite precipitated during the heating of seawater will be permanently sequestered in the crust but it seems more likely anhydrite dissolves as the system cools adding these components back into the ocean; this would increase the difference in the total hydrothermal Ca flux between modern and Cretaceous. For example, using their model but assuming that anhydrite subsequently dissolves, leads to a modern net loss of Ca from the crust of 53 mmol kg^{-1} of vent fluid as compared to 30 mmol for their Cretaceous model; i.e. a 75% increase in the Ca flux (data from their Fig. 2). Importantly, in this scenario the Ca flux from the crust matches the Mg flux carried by seawater into the crust (e.g., Berner et al., 1983), providing a negative feedback on changes in the Mg/Ca of seawater. In summary, while high-temperature reactions are largely rock-buffered, changes in the major ion chemistry of seawater probably affect the role of anhydrite in oceanic hydrothermal systems and its role in influencing the behavior of other species deserves further work.

3.3. The role of ocean chemistry and temperature in low-temperature mixing

In this section we consider how the composition and temperature of ocean bottom water affects the net hydrothermal flux due to reactions during mixing both below and above the seafloor. Conservative elements, such as the alkalis, are not affected by mixing processes and their net flux simply depends on the extent of leaching from the crust.

3.3.1. Sulfate precipitation during discharge and the partitioning of diffuse versus focussed flow

The sulfate concentration in seawater is thought to have varied by a factor of three or more over the Phanerozoic (e.g., Lowenstein et al., 2014). This is likely to have changed the extent of sulfate mineral precipitation during mixing of discharging high-temperature hydrothermal fluids and seawater. The alkaline earth elements can form sulfate minerals precipitated during mixing of upwelling hydrothermal fluids and seawater-like fluids either below or above the seafloor. The main sulfate minerals are anhydrite and barite although Mg-hydroxy-sulfate-hydrate (MHSH; caminite) may form under some circumstances (e.g., Antonelli et al., 2017; Bischoff and Seyfried, 1978; Mottl et al., 1979; Seyfried and Bischoff, 1981; Haymon and Kastner, 1986). Precipitation of sulfates during mixing decreases the net flux of alkaline earth elements directly into the ocean although anhydrite probably largely re-dissolves as the system cools. Formation and/or dissolution of these phases could also substantially affect the on-axis permeability structure of the crust. When seawater sulfate concentrations were lower than that of the modern ocean (e.g., early Paleozoic and Cretaceous), less anhydrite would have precipitated within the crust (and perhaps at the seafloor in chimneys too). Anhydrite precipitation in the subsurface decreases permeability, and likely helps focus high-temperature fluid channelization through, and out of, the lava pile (e.g., Haymon, 1983; Sleep, 1991; Lowell et al., 2003). The fraction of the hydrothermal flux discharged at focused vents ("black smokers") may therefore have varied substantially over the Phanerozoic. This would also affect the fluxes associated with hydrothermal plumes. For example, the negative fluxes (i.e., out of seawater) of those elements co-precipitated with, or scavenged by, hydrothermal particles (e.g., oxyanions, REEs) could have been lower at times of lower seawater sulfate.

3.3.2. Iron oxidation and dispersal in the hydrothermal plume

Changes in the temperature, pH, oxygen content and abundance of different organic ligands in the deep ocean also affect processes operating in hydrothermal plumes. The formation of Fe-oxyhydroxides during mixing of seawater and hydrothermal fluids, and during oxidative dissolution of particulate sulfides within the hydrothermal plume, depend on the kinetics of oxidation of both dissolved Fe^{2+} and nanoparticle sulfide as well as the solubility of Fe^{3+} in seawater. The rate of dissolved iron oxidation increases with increasing temperature, dissolved O_2 and pH, and decreasing salinity (Millero et al., 1987). Because of the high dilution factors in the neutrally buoyant plume, these controlling parameters are largely set by the composition of bottom water. The range of these parameters in the modern deep ocean predicts a ~20 fold variation in the half-life of dissolved Fe^{2+} (Field and Sherrell, 2000), and substantially larger changes might be expected over Earth history. The oxidation rate of pyrite nanoparticles within a hydrothermal plume also depends on the oxygen content, temperature, and pH of bottom water, with pyrite nanoparticles having calculated half-lifes of ~0.5 to 2 years in the modern ocean basins dependent on bottom water O_2 (Gartman and Luther, 2014). Faster Fe oxidation is expected to lead to a shorter residence time for Fe in the neutrally buoyant plume, potentially providing less Fe to the far-field ocean where it can act as a micronutrient (e.g., Tagliabue et al., 2010). Further, the net scavenging flux associated with particulate Fe-oxyhydroxides is expected to generally be smaller if particles are more rapidly sedimented. Finally, the solubility of Fe^{3+} affects far field transport of

Fe in hydrothermal plumes (e.g., Fitzsimmons et al., 2017). In seawater Fe^{3+} solubility depends on temperature, pH and salinity but, across the likely range of these parameters in Phanerozoic seawater, the abundance of organic ligands that can form aqueous Fe-complexes may be more important (e.g., Liu and Millero, 2002; Gledhill and van den Berg, 1994).

4. Examples of axial hydrothermal flux variability

To place the conceptual models linking environmental conditions to hydrothermal fluxes presented above in more context this section provides two examples of how hydrothermal fluxes may have changed over different periods of Earth history. The first concerns potential changes in hydrothermal fluxes over Quaternary glacial-interglacial cycles due to changes in sea level and bottom water temperature and composition. The second explores how the major ion chemistry of seawater may have modified hydrothermal fluxes over the Phanerozoic.

4.1. Axial hydrothermal fluxes over glacial-interglacial cycles

Quaternary glacial-interglacial (G-IG) cycles have been accompanied by substantial changes in sea level and bottom water conditions which are expected to have impacted global hydrothermal fluxes. Interglacial periods are characterized by higher sea level which is expected to lead to higher peak hydrothermal fluid temperatures (Fig. 5) and higher pressure phase separation producing, on average, a more Cl-rich vapor (Figs. 3, 6). In combination, these effects are predicted to have led to higher concentrations of many elements (e.g., Li, Mn, Fe, Zn, As, Rb, Cs) in upwelling, high-temperature, hydrothermal fluids (Section 3.1; Figs. 4, 5). Changes in high-temperature fluid compositions of the order of 50 to 100% appear plausible for elements like Fe and Mn, although the values are not well constrained, and changes in the net flux across the seafloor may be smaller for non-conservative elements. Small additional changes in vent fluid composition are also expected from the change in ocean salinity over G-IG cycles (Section 3.2.1). Due to pressure effects, the average upwelling high-temperature hydrothermal fluid will have had a higher Fe/H_2S during interglacials than glacials which will have led to a larger fraction of the Fe in the hydrothermal plume being housed in Fe-oxyhyroxides than Fe-sulfides.

Changes in bottom water chemistry and temperature across G-IG cycles also occurred due to climatic fluctuations and changes in ocean circulation and biogeochemical cycling (e.g., Mills et al., 2010; Yu et al., 2013; Rae et al., 2014; Galbraith and Jaccard, 2015). Interglacial periods are characterized by lower salinity and warmer bottom water. Additionally, changes in bottom water pH and O_2 are expected, although the details vary with location and are currently generally not well constrained (Yu et al., 2013; Rae et al., 2014; Galbraith and Jaccard, 2015). Changes in bottom water temperature, salinity, pH and O_2 are predicted to lead to hydrothermal plumes behaving substantially differently during glacial and interglacial periods. For example, Cullen and Coogan (2017) argue that changes in bottom water chemistry above the equatorial East Pacific Rise during the transition from the last glacial to the current interglacial should have led to a large increase in the rate of Fe oxidation in hydrothermal plumes. Such an increase in Fe-oxidation rate is expected to increase the rate of sedimentation of Fe from the plume and reduce the fraction of Fe exported far from the ridge axis. Likewise, significant variation in Fe-sulfide oxidation rates are expected between glacial and interglacial times. Additionally, changes in deep ocean stratification could have led to variation in plume rise heights (e.g., Speer and Rona, 1989) and, along with variation in deep ocean currents, modified the dispersal of hydrothermal material.

The hypothesized G-IG changes in both the composition of high-temperature hydrothermal fluids, and in hydrothermal plume processes, can potentially be tested against archives of hydrothermal element fluxes into the ocean. The best existing records come in the accumulation rate of hydrothermally contributed components in sediments around mid-ocean ridges. Strong enrichments in hydrothermally derived components (e.g., Fe, Mn) at glacial-interglacial transitions have been observed in some, but not all, near-ridge sediment cores. These data have been interpreted in different ways including: (i) changes in the extent of mantle melting, and hence melt supply to the crust, changing the hydrothermal fluid flux (Lund and Asimow, 2011; Lund et al., 2016; Middleton et al., 2016; Costa et al., 2017); and (ii) changes in the redox state of the deep ocean affecting element mobilization from sediments during diagenesis and/or redeposition (Mangini et al., 1990; Frank et al., 1994; Schaller et al., 2000; Mills et al., 2010; Costa et al., 2018). However, changes in the response of oceanic hydrothermal systems to changing ocean depth and/or bottom water chemistry as described above are also plausible hypotheses that are perhaps better able to explain the large magnitude of the signal (Kump and Seyfried, 2005; Cullen and Coogan, 2017; Pester, 2018; Section 3.1.2). Further testing between these alternatives will require more robust models and datasets.

If either the average composition of hydrothermal fluids, or particle formation and sedimentation rates, changed over G-IG cycles this could have implications for ocean biogeochemical cycles. For example, an increase in the fraction of the Fe that was deposited close to the ridge axis could have led to a decrease in the extent of hydrothermal Fe fertilization of the ocean. Alternatively, an increase in the Fe content of hydrothermal fluids could have the inverse effect (Kump and Seyfried, 2005; Middleton et al., 2016). Likewise, if more hydrothermal Fe is taken up in Fe-oxyhydroxides (due to either higher Fe/H_2S of vent fluids or changes in Fe oxidation rate in the abyssal ocean) then more phosphorous could get scavenged by these particles, decreasing the availability of this essential nutrient. While such effects are speculative, such potential feedbacks between oceanic hydrothermal fluxes and environment conditions warrant further investigation.

4.2. Axial hydrothermal flux variability over the Phanerozoic

There is substantial evidence that there have been large changes in both ocean depth and seawater major ion chemistry over the Phanerozoic, although the details are uncertain. To illustrate the potential for these changes to affect hydrothermal fluxes we briefly consider the impact of: (i) changes in ocean salinity (Hay et al., 2006); (ii) changes in the Mg-Ca-sulfate content of seawater (e.g., Hardie, 1996; Lowenstein et al., 2014); and (iii) changes in sea level (e.g., Miller et al., 2005; Müller et al., 2008). Based on the discussion in Section 3 we parameterized changes in the hydrothermal flux of Ca relative to the modern as functions of these controlling variables. There are large uncertainties in these parameterizations and they should be considered preliminary.

4.2.1. Changing seawater salinity

Changes in the salinity of the seawater will affect the hydrothermal Ca flux through the mineral-fluid equilibria described by Eq. (1) (Berndt and Seyfried, 1993; Seyfried et al., 2002; Pester et al., 2015) which has an equilibrium constant:

$$K_{eq} = (a^2_{albite} a_{CaCl_2})/(a^4_{SiO_2} a_{anorthite} a^2_{NaCl}) \quad (2)$$

Because (hydrothermal) quartz and metastable plagioclase solid solutions are generally present in altered sheeted dikes, changes in seawater NaCl content should lead to changes in the Ca content of the hydrothermal fluid:

$$CaCl_{2HF} \propto NaCl^2_{SW} \quad (3)$$

where subscripts *HF* and *SW* represent the hydrothermal fluid and seawater respectively. Using as reference points the salinity of modern seawater ($NaCl_{SW}{}^0$), and the predicted Ca content of he average modern hydrothermal fluid ($Ca_{HF}{}^0 = 35\ mmol\ kg^{-1}$, Fig. 7 inset), we can write

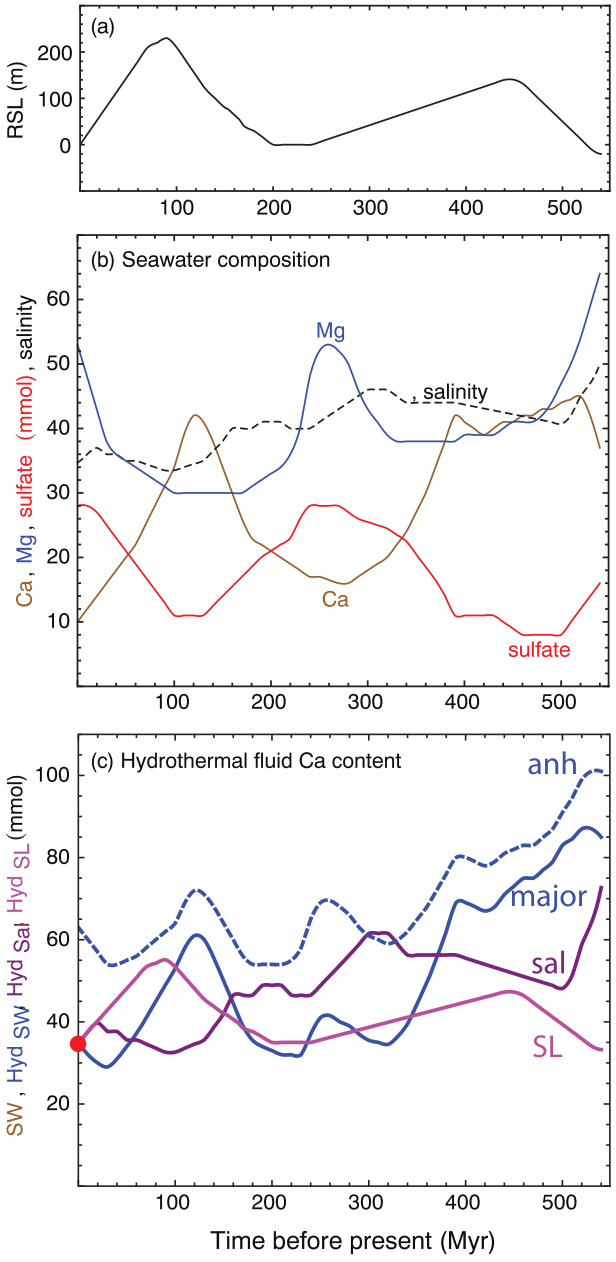

Fig. 8. Approximate variation in Phanerozoic: (a) sea level relative to modern (Exxon curve from Miller et al., 2005); (b) seawater major ion content (Ca and sulfate from Lowenstein et al., 2003; Mg from Antonelli et al., 2017) and salinity (Hay et al., 2006); and (c) model Ca content of high-temperature hydrothermal fluids based on parameterizations of the response of the hydrothermal system to the variations shown in parts (a) and (b). The red dot is the estimated modern hydrothermal vent fluid Ca content and the curves labeled SL, Sal, maj and anh show the model vent fluid composition calculated assuming just the effect of changing sea level, seawater salinity, seawater major ion content assuming anhydrite remains trapped in the crust and seawater major ion content assuming anhydrite dissolves in the off-axis (dashed curve), respectively. See text for caveats regarding model simplifications and uncertainties.

an equation relating the hydrothermal vent fluid Ca at any time in the past ($Ca^t_{HF(salinity)}$) to the salinity of the ocean at that time ($NaCl^t_{SW}$):

$$Ca^t_{HF(salinity)} = [Ca^0_{HF}]\frac{[NaCl^t_{SW}]^2}{[NaCl^0_{SW}]^2} \quad (4)$$

While Eq. (4) is a simplification, and ignores the effects of phase separation (see above), it provides a simple illustration of the potential effect of changing ocean salinity on hydrothermal Ca fluxes (Figs. 7, 8).

Using the secular variation in seawater salinity from Hay et al. (2006), Eq. (4) predicts approximately a factor of two variation in the Ca content of hydrothermal fluids over the Phanerozoic solely due to changes in ocean salinity (Fig. 8c). This scale of variability is sufficient that it may have played a role in the evolution of ocean chemistry. Likewise, changes in the hydrothermal flux of other elements due to changing seawater salinity may also be important in the evolution of ocean chemistry over the Phanerozoic.

4.2.2. Changing seawater major ion composition

Following Antonelli et al. (2017), and noting the caveats about this model made in Section 3.2.2, we assume that Ca and sulfate in seawater are precipitated upon heating during recharge until all of sulfate is consumed. If the Ca content of seawater is lower than that of sulfate the deficit is made up by leaching Ca from the rock in exchange for Mg at a 1:1 ratio. Further Ca−Mg exchange occurs until all Mg is lost from the fluid. In this case the hydrothermal fluid Ca content at any given seawater major element composition is:

$$Ca^t_{HF(major)} = Ca_{SW} + Mg_{SW} - SO_4^{SW} \quad (5)$$

where all terms are in molar units. If all anhydrite dissolves in the off-axis, the net flux of Ca into the ocean equals the net flux of Mg into the crust.

The variation in hydrothermal Ca flux predicted by the model of Antonelli et al. (2017) over the Phanerozoic is a factor of two (assuming anhydrite dissolution) to a factor of three (assuming no anhydrite dissolution). As discussed above, Eq. (5) is a substantial simplification of the charge balance constraints, with Fe and K being important components that need considering in future models, along with Ca−Na exchange equilibria (Eq. (1)) and the charge balance of the initial seawater composition. The reaction path models of Antonelli et al. (2017; their Supplementary Fig. 1) suggest that the magnitude of variation in hydrothermal fluid Ca flux shown in Fig. 8 due to variation in seawater major ion composition over the Phanerozoic is probably an over-estimate.

4.2.3. Changing sea level

Changes in sea level over the Phanerozoic could have led to variation in hydrothermal fluxes in different ways (Section 3.1). As an example we consider changes in the Ca flux due to the effect of sea level on phase separation processes (discussed in Section 3.1.2). At typical hydrostatic pressures near the base of hydrothermal systems along modern fast-spreading ridges the mass fraction of vapor increases ~3%, and its NaCl content increases ~0.15 wt%, for every 100 m increase in sea level (Fig. 6). At the same time, the liquid NaCl content increases ~0.7 wt% per 100 m increase in sea level (Fig. 6). The change in the vapor Ca content can be calculated from experimentally derived partitioning data (e.g., Pester et al., 2015):

$$Log[Ca_v/Ca_l] = 1.35Log[Cl_v/Cl_l] \quad (6)$$

where, v = vapor, l = liquid. Using the results given in Fig. 6, Ca_v/Ca_l increases from 0.046 to 0.063 between 32 and 35 MPa and the mass fraction of vapor increases from 72 to 82%. In combination these changes lead to the fraction of the Ca stored in the vapor increasing from ~0.15 to ~0.27 (an 86% increase). Based on this we parameterize the change in Ca content of the hydrothermal fluid due to changing sea level as:

$$Ca^t_{HF(SL)} = Ca^0_{HF} + 0.86[Ca^0_{HF}]\left(\frac{\Delta SL}{300}\right) \quad (7)$$

where $Ca^t_{HF(SL)}$ is the hydrothermal fluid Ca content for any given sea level change and ΔSL is the change in sea level relative to modern (in meters). Eq. (7) represents, at best, a very preliminary parameterization of the change in hydrothermal flux with changing sea level but is used here for illustrative purposes.

The change in hydrothermal Ca flux predicted by Eq. (7) is of the

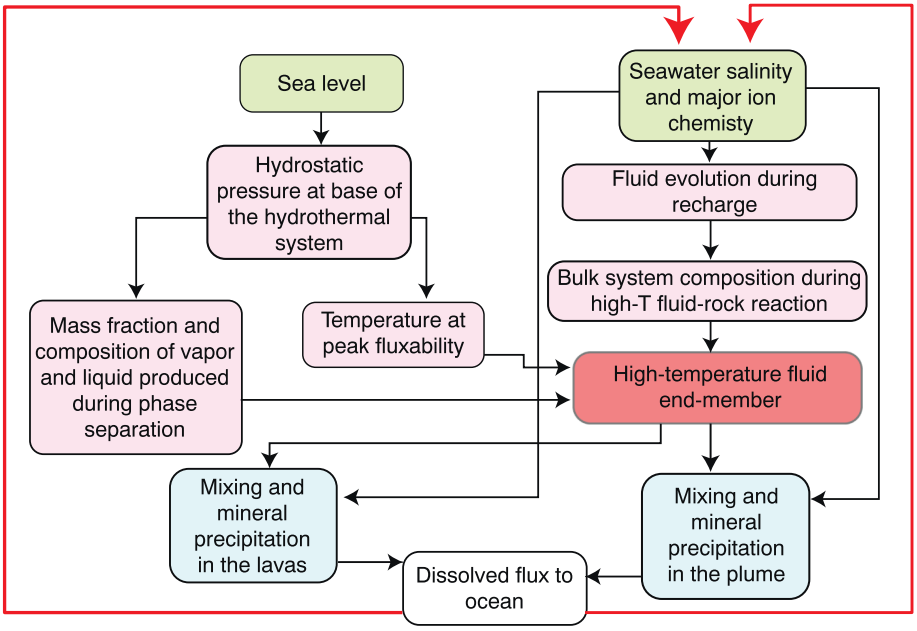

Fig. 9. Flow chart summarizing ways in which changes in sea level and ocean major ion composition can impact high temperature hydrothermal fluxes. Changes in geodynamic boundary conditions (e.g., global rate of oceanic crustal production, average crustal thickness and stage in the Wilson cycle; Section 2.1) operate as a further layer of control on hydrothermal fluxes.

same order, although somewhat smaller, than those predicted due to changes in seawater salinity and major ion compositions. Considering the uncertainties in all the parameterizations (Eqs. (4), (5) and (7)) we caution that the absolute concentrations of Ca in paleo-hydrothermal fluids shown in Fig. 8c are subject to large uncertainties. However, we consider it unlikely that all of the parameterizations substantially overestimate the effects and thus we suggest that it is likely that high-temperature hydrothermal fluxes have varied substantially over the Phanerozoic, independent of crustal accretion rate. With the uncertainties in absolute fluxes in mind, it is useful to place this variability in a broader context. Assuming a high-temperature hydrothermal fluid flux of $\sim 8 \times 10^{12}$ kg yr^{-1} (Coogan and Dosso, 2012) the results shown in Fig. 8c give a range of hydrothermal Ca fluxes into the ocean over the Phanerozoic of 0.25 to 0.8 Tmol yr^{-1}. This is equivalent to ~20 to 60% of the modern river Ca flux that comes from dissolving silicates (i.e., ignoring the riverine Ca from carbonate weathering; Gaillardet et al., 1999). Changes of this magnitude are clearly non-trivial for ocean chemistry.

5. Future research directions

While much is known about the fundamental controls on the composition of high-temperature hydrothermal fluids we have few quantitative constraints on how the net fluxes between the ocean and oceanic crust in these systems vary with changing environmental conditions. More robust parameterizations of hydrothermal fluxes in terms of environmental conditions, that will allow more robust models of the evolution of ocean chemistry, will be facilitated by future work such as:

- Studies of the rock record to determine if there is evidence for changing hydrothermal fluxes associated with on-axis hydrothermal systems as predicted here. For example, do the compositions of fluid inclusions trapped at high-temperatures (~400 °C) vary with the age of crust they are trapped in? Likewise, do hydrothermal sediments record changes in hydrothermal fluxes due to changing environmental conditions?
- Further investigation into the role of anhydrite in axial hydrothermal systems.
- Further experimental studies, and development of thermodynamic data, for minerals and fluids at conditions near peak fluxability (i.e., near the two-phase curve; Fig. 3), and for fluids decompressing near adiabatically from these conditions. In particular, further studies to assess how relatively small pressure changes, such as those due to changing sea level (and consequent temperature changes), affect element mobility will be useful.
- Development of reactive transport models that integrate field and laboratory results and allow exploration of the roles of key variables (permeability, reaction kinetics) in controlling model hydrothermal fluxes under different environmental conditions (seawater composition, hydrostatic pressure).
- Construction of more comprehensive, and better calibrated, models of the role of seawater composition and temperature in the modification of hydrothermal fluxes during sub- and supra-surface mixing, mineral precipitation and sedimentation.
- Field studies to better understand the partitioning of the hydrothermal flux between high- temperature and diffuse discharge and to address the role of “intermediate” temperature fluids. Such intermediate temperature fluids may form by fluid circulation at temperatures well below that of peak fluxability (e.g., 200 °C) for example during times of low axial heat flux where no surficial vents are evident and there is no water column plume. Such fluids are poorly understood but there is evidence that they may be important in global ocean chemical cycles (e.g., de Villiers, 1998).

6. Summary and conclusions

Potential links between environmental conditions and high-temperature, on-axis, hydrothermal fluxes are summarized in Fig. 9. Changes in global sea level change the pressure near the base of axial hydrothermal systems changing both the temperature at which the fluid most efficiently extracts heat (Fig. 3d) and the compositions and mass fractions of vapor and liquid produced during phase separation (Figs. 3, 6). Both of these have the potential to lead to changes in the net hydrothermal chemical flux. Changes in ocean chemistry can change the behavior of axial hydrothermal systems in numerous ways. Perhaps most important, changes in seawater salinity will change the phase equilibria such that, in general, element fluxes into the ocean will increase with increasing seawater salinity. Seawater sulfate content plays an important role in oceanic hydrothermal system through the precipitation of anhydrite in the crust which modifies crustal porosity and permeability in the shallow portions of both the recharge and discharge zones. Additionally, seawater sulfate modifies the behavior of Ca and Sr

in the recharge zone (Antonelli et al., 2017). Seawater Mg is almost completely lost to the crust providing a negative feedback on increases in seawater Mg. Seawater chemistry also affects net hydrothermal fluxes through its dominant role in controlling the bulk fluid composition in hydrothermal plumes and during sub-surface mixing. Here changes in seawater composition can control what phases form, the kinetics of both mineral formation and dissolution and the flux of elements out of the ocean due to co-precipitation and scavenging.

The links between environmental conditions and axial hydrothermal fluxes described above suggest that axial hydrothermal fluxes are highly likely to vary with environmental conditions. However, there is substantial uncertainty in quantifying these links and we hope this contribution inspires further work in this area. Indeed, this contribution is, as much as anything, a plea for greater consideration of both the magnitude and variability in axial hydrothermal chemical fluxes and how these may interact with ocean chemistry. Continued use of constant "book values" from easily accessible tabulations, without critical evaluation, will hinder progress in understanding the history of ocean chemistry and what this tells us about the Earth system.

Acknowledgements

Jeff Alt, Lee Kump and an anonymous reviewer are thanked for their comments which helped improved the manuscript. Jay Cullen is thanked for numerous discussions that have helped shape LAC's thinking about the evolution of hydrothermal plume processes over Earth history. Drew Syverson and Ben Tutolo are thanked for inviting LAC to present in their hydrothermal session at Goldschmidt 2017 which acted as the catalyst for the writing of this manuscript.

References

Alt, J.C., 1995. Seafloor processes in mid-ocean ridge hydrothermal systems. In: Humphris, S.E., Zierenberg, R.A., Millineaux, L.S., Thomson, R.E. (Eds.), Seafloor Hydrothermal Systems: Physical, Chemical, Biological, and Geological Interactions. Am. Geophys. Un, Washington, D.C., pp. 85–114.

Alt, J.C., Anderson, T.F., Bonnell, L., 1989. The geochemistry of sulfur in a 1.3 km section of hydrothermally altered oceanic crust, DSDP Hole 504B. Geochim. Cosmochim. Acta 53, 1011–1023.

Alt, J.C., Davidson, G.J., Teagle, D.A.H., Karson, J.A., 2003. Isotopic composition of gypsum in the Macquarie Island ophiolite: implications for the sulfur cycle and the subsurface biosphere in oceanic crust. Geology 31, 549–552.

Alt, J.C., Laverne, C., Coggon, R.M., Teagle, D.A.H., Banerjee, N.R., Morgan, S., Smith-Duque, C.E., Harris, M., Galli, L., 2010. Subsurface structure of a submarine hydrothermal system in ocean crust formed at the East Pacific Rise, ODP/IODP Site 1256. Geochemistry Geophys. Geosystems 11. https://doi.org/10.1029/2010GC003144.

Antonelli, M.A., Pester, N.J., Brown, S.T., DePaolo, D.J., 2017. Effect of paleoseawater composition on hydrothermal exchange in midocean ridges. Proc. Natl. Acad. Sci. 114, 12413–12418.

Bach, W., Klein, F., 2009. The petrology of seafloor rodingites: insights from geochemical reaction path modeling. Lithos 112, 103–117.

Baker, E.T., Massoth, G.J., 1987. Characteristics of hydrothermal plumes from two vent fields on the Juan de Fuca Ridge, northeast Pacific Ocean. Earth Planet. Sci. Lett. 85, 59–73.

Baker, E.T., Chen, Y.J., Phipps Morgan, J., 1996. The relationship between near-axis hydrothermal cooling and the spreading rate of mid-ocean ridges. Earth Planet. Sci. Lett. 142, 137–145.

Baker, E.T., Edmonds, H.N., Michael, P.J., Bach, W., Dick, H.J.B., Snow, J.E., Walker, S.L., Banerjee, N.R., Langmuir, C.H., 2004. Hydrothermal venting in magma deserts: the ultraslow spreading Gakkel and Southwest Indian Ridges. Geochemistry Geophys. Geosystems 5, 2004GC000712.

Barker, A.K., Coogan, L.A., Gillis, K.M., Weis, D., 2008. Strontium isotope constraints on fluid flow in the sheeted dike complex of fast spreading crust: pervasive fluid flow at Pito Deep. Geochemistry Geophys. Geosystems. https://doi.org/10.1029/2007GC001901.

Barker, A.K., Coogan, L.A., Gillis, K.M., 2010. Insights into the behaviour of sulphur in mid-ocean ridge axial hydrothermal systems from the composition of the sheeted dyke complex at Pito Deep. Chem. Geol. 275, 105–115.

Bekker, A., Planavsky, N.J., Krapež, B., Rasmussen, B., Hofmann, A., Slack, J.F., Rouxel, O.J., Konhauser, K.O., 2014. 9.18 - iron formations: their origins and implications for ancient seawater chemistry. In: Holland, H.D., Turekian, K.K. (Eds.), Treatise on Geochemistry, Second edition. Elsevier, Oxford, pp. 561–628.

Berndt, M.E., Seyfried, W.E., 1997. Calibration of BrCl fractionation during subcritical phase separation of seawater: possible halite at 9 to 10°N East Pacific Rise. Geochim. Cosmochim. Acta 61, 2849–2854.

Berndt, M.E., Seyfried Jr., W.E., 1993. Calcium and sodium exchange during hydrothermal alteration of calcic plagioclase at 400°C and 400 bars. Geochim. Cosmochim. Acta 57, 4445–4451.

Berndt, M.E., Seyfried Jr., W.E., Beck, J.W., 1988. Hydrothermal alteration processes at Midocean Ridges: experimental and theoretical constraints from Ca and Sr exchange reactions and Sr isotopic ratios. Jour. Geophys. Res. 93, 4573–4583.

Berner, R.A., Lasaga, A.C., Garrels, R.M., 1983. The carbonate-silicate geochemical cycle and its effect on atmospheric carbon dioxide over the past 100 million years. Am. J. Sci. 283, 641–683.

Bickle, M.J., Teagle, D.A.H., 1992. Strontium alteration in the Troodos ophiolite: implications for fluid fluxes and geochemical transport in mid-ocean ridge hydrothermal systems. Earth Planet. Sci. Lett. 113, 219–237.

Bischoff, J.L., 1991. Densities of liquids and vapors in boiling NaCl-H_2O solutions: a PVTx summary from 300° to 500°C. Am. J. Sci. 291, 309–338.

Bischoff, J.L., Dickson, F.W., 1975. Seawater-basalt interaction at 200°C and 500 bars: implications for origin of sea-floor heavy-metal deposits and regulation of seawater chemistry. Earth Planet. Sci. Lett. 25, 385–397.

Bischoff, J.S., Pitzer, K., 1989. Liquid-vapor relations for the system NaCl-H_2O: summary of the P-T-X surface from 300°C to 500°C. Am. J. Sci. 289, 217–248.

Bischoff, J.L., Rosenbauer, R.J., 1985. An empirical equation of state for hydrothermal seawater (3.2 percent NaCl). Amer. J. Sci. 285, 725–763.

Bischoff, J.L., Rosenbauer, R.J., 1987. Phase separation in seafloor geothermal systems: an experimental study of the effects on metal transport. Am. Jour. Sci. 287, 953–978.

Bischoff, J.L., Rosenbauer, R.J., 1989. Salinity variations in submarine hydrothermal systems by layered double-diffusive convection. J. Geol. 97, 613–623.

Bischoff, J.L., Seyfried Jr., W.E., 1978. Hydrothermal chemistry of seawater from ˚C to 350°C. Am. J. Sci. 278, 838–860.

Boström, K., Peterson, M.N.A., Joensuu, O., Fisher, D.E., 1969. Aluminum-poor ferromanganoan sediments on active oceanic ridges. J. Geophys. Res. 74, 3261–3270.

Butterfield, D.A., Mcduff, R.E., Mottl, M.J., Lilley, M.D., Lupton, J.E., Massoth, G.J., 1994. Gradients in the composition of hydrothermal fluids from the endeavor segment vent field - phase-separation and brine loss. J. Geophys. Res. Earth 99, 9561–9583.

Butterfield, D.A., Jonasson, I.R., Massoth, G.J., Feely, R.A., Roe, K.K., Embley, R.E., Holden, J.F., McDuff, R.E., Lilley, M.D., Delaney, J.R., 1997. Seafloor eruptions and evolution of hydrothermal fluid chemistry. Phil. Trans. R. Soc. Lon. A 355, 369–386.

Cann, J.R., Gillis, K.M., 2004. Hydrothermal insights from the Troodos ophiolite, Cyprus. In: Elderfield, H., Davis, E. (Eds.), The Hydrology of the Oceanic Lithosphere. Cambridge university press.

Cannat, M., 1993. Emplacement of mantle rocks in the seafloor at mid-ocean ridges. Jour. Gephys. Res. 98, 4163–4172.

Chan, L.-H., Alt, J.C., Teagle, D.A.H., 2002. Lithium and lithium isotope profiles through the upper oceanic crust: a study of seawater-basalt exchange at ODP Sites 504B and 896A. Earth Planet. Sci. Lett. 201, 187–201.

Charlou, J.L., Donval, J.P., Fouquet, Y., Jean-Baptiste, P., Holm, N., 2002. Geochemistry of high H2 and CH4 vent fluids issuing from ultramafic rocks at the rainbow hydrothermal field (36°14'N, MAR). Chem. Geol. 191, 345–359.

Chavagnac, V., Ali, H.S., Jeandel, C., Leleu, T., Destrigneville, C., Castillo, A., Cotte, L., Waeles, M., Cathalot, C., Laes-Huon, A., Pelleter, E., Nonnotte, P., Sarradin, P.-M., Cannat, M., 2018. Sulfate minerals control dissolved rare earth element flux and Nd isotope signature of buoyant hydrothermal plume (EMSO-Azores, 37°N Mid-Atlantic Ridge). Chem. Geol. 499, 111–125.

Chin, C.S., Coale, K.H., Elrod, V.A., Johnson, K.S., Massoth, G.J., Baker, E.T., 1994. In situ observations of dissolved iron and manganese in hydrothermal vent plumes, Juan de Fuca Ridge. J. Geophys. Res. 99, 4969–4984.

Coogan, L.A., 2008. Reconciling temperatures of metamorphism, fluid fluxes and heat transport in the upper crust at intermediate- to fast-spreading mid-ocean ridges. Geochemistry Geophys. Geosystems. 9, Q02013. https://doi.org/10.1029/2007GC001787.

Coogan, L.A., Dosso, S., 2012. An internally consistent, probabilistic, determination of ridge-axis hydrothermal fluxes from basalt-hosted systems. Earth Planet. Sci. Lett. 323, 92–101.

Coogan, L.A., Attar, A., Mihaly, S.F., Jeffries, M., Pope, M., 2017. Near-vent chemical processes in a hydrothermal plume: Insights from an integrated study of the Endeavour segment. Geochemistry, Geophys. Geosystems 18, 1641–1660. https://doi.org/10.1002/2016GC006747.

Cooper, M.J., Elderfield, H., Schultz, A., 2000. Diffuse hydrothermal fluids from Lucky Strike hydrothermal vent field: evidence for a shallow conductively heated system. Jour. Geophys. Res. 105, 19,369–19375.

Costa, K.M., McManus, J.F., Middleton, J.L., Langmuir, C.H., Huybers, P.J., Winckler, G., Mukhopadhyay, S., 2017. Hydrothermal deposition on the Juan de Fuca Ridge over multiple glacial–interglacial cycles. Earth Planet. Sci. Lett. 479, 120–132.

Costa, K.M., Anderson, R.F., McManus, J.F., Winckler, G., Middleton, J.L., Langmuir, C.H., 2018. Trace element (Mn, Zn, Ni, V) and authigenic uranium (aU) geochemistry reveal sedimentary redox history on the Juan de Fuca Ridge, North Pacific Ocean. Geochim. Cosmochim. Acta 236, 79–98.

Coumou, D., Driesner, T., Heinrich, C.A., 2008. The structure and dynamics of mid-ocean ridge hydrothermal systems. Science 321, 1825–1828.

Coumou, D., Driesner, T., Geiger, S., Paluszny, A., Heinrich, C.A., 2009a. High-resolution three-dimensional simulations of mid-ocean ridge hydrothermal systems. J. Geophys. Res. 114, B07104. https://doi.org/10.1029/2008JB006121.

Coumou, D., Driesner, T., Weis, P., Heinrich, C.A., 2009b. Phase separation, brine formation, and salinity variation at Black Smoker hydrothermal systems. J. Geophys. Res. 114, B03212. https://doi.org/10.1029/2008JB005764.

Cruse, A.M., Seewald, J.S., 2006. Geochemistry of low-molecular weight hydrocarbons in hydrothermal fluids from Middle Valley, northern Juan de Fuca Ridge. Geochim. Cosmochim. Acta 70, 2073–2092.

Cullen, J.T., Coogan, L.A., 2017. Changes in Fe oxidation rate in hydrothermal plumes as

a potential driver of enhanced hydrothermal input to near-ridge sediments during glacial terminations. Geophys. Res. Lett. 44. https://doi.org/10.1002/2017GL074609.
de Villiers, S., 1998. Excess dissolved Ca in the deep ocean: a hydrothermal hypothesis. Earth Planet. Sci. Lett. 164, 627–641.
Demicco, R.V., Lowenstein, T.K., Hardie, L.A., Spencer, R.J., 2005. Model of seawater composition for the Phanerozoic. Geology 33, 877–880.
Ding, K., Seyfried, W.E., 1992. Determination of Fe-Cl complexing in the low-pressure supercritical region (NaCl fluid) - iron solubility constraints on pH of subseafloor hydrothermal fluids. Geochim. Cosmochim. Acta 56, 3681–3692.
Douville, E., Charlou, J.L., Oelkers, E.H., Bienvenu, P., Jove Colon, C.F., Donval, J.P., Fouquet, Y., Prieur, D., Appriou, P., 2002. The rainbow vent fluids (36°14'N, MAR): the influence of ultramafic rocks and phase separation on trace metal content in Mid-Atlantic Ridge hydrothermal fluids. Chem. Geol. 184, 37–48.
Driesner, T., 2007. The system H_2O-NaCl Part II: correlations for molar volume, enthalpy, and isobaric heat capacity from 0 to 1000°C, 0 to 5000 bar, and 0 to 1 XNaCl. Geochim. Cosmochim. Acta 71, 4902–4919.
Driesner, T., Heinrich, C.A., 2007. The system H_2O–NaCl. Part I: correlation formulae for phase relations in temperature–pressure–composition space from 0 to 1000°C, 0 to 5000bar, and 0 to 1 XNaCl. Geochim. Cosmochim. Acta 71, 4880–4901.
Dymond, J., Corliss, J.B., Heath, G.R., 1977. History of metalliferous sedimentation at deep sea drilling site 319 in the South Eastern Pacific. Geochim. Cosmochim. Acta 41, 741–753.
Elderfield, H., Schultz, A., 1996. Mid-ocean ridge hydrothermal fluxes and the chemical composition of the ocean. Annu. Rev. Earth Planet. Sci. 24, 191–224.
Feely, R.A., Geiselman, T.L., Baker, E.T., Massoth, G.J., Hammond, S.R., 1990. Distribution and composition of hydrothermal plume particles from the ASHES Vent Field at Axial Volcano, Juan de Fuca Ridge. J. Geophys. Res. Solid Earth 95, 12855–12873.
Feely, R.A., Massoth, G.J., Baker, E.T., Lebon, G.T., Geiselman, T.L., 1992. Tracking the dispersal of hydrothermal plumes from the Juan de Fuca Ridge using suspended matter compositions. J. Geophys. Res. Solid Earth 97, 3457–3468.
Field, M.P., Sherrell, R.M., 2000. Dissolved and particulate Fe in a hydrothermal plume at 9°45′N, East Pacific Rise: slow Fe (II) oxidation kinetics in Pacific plumes. Geochim. Cosmochim. Acta 64, 619–628.
Fitzsimmons, J.N., John, S.G., Marsay, C.M., Hoffman, C.L., Nicholas, S.L., Toner, B.M., German, C.R., Sherrell, R.M., 2017. Iron persistence in a distal hydrothermal plume supported by dissolved-particulate exchange. Nat. Geosci. 10, 195–201.
Fontaine, F.J., Wilcock, W.S.D., 2006. Dynamics and storage of brine in mid-ocean ridge hydrothermal systems. J. Geophys. Res. 11. https://doi.org/10.1029/2005JB003866.
Fontaine, F.J., Wilcock, W.S.D., 2007. Physical controls on the salinity of mid-ocean ridge hydrothermal vent fluids. Earth Planet. Sci. Lett. 257, 132–145.
Fouquet, Y., Zierenberg, R.A., Miller, D.J., 1998. Proc. ODP, Init. Repts., 169. Ocean Drilling Program, College Station, Texas.
Foustoukos, D.I., Seyfried, W.E., 2007. Trace element partitioning between vapor, brine and halite under extreme phase separation conditions. Geochim. Cosmochim. Acta 71, 2056–2071.
Foustoukos, D.I., Pester, N.J., Ding, K., Seyfried Jr., W.E., 2009. Dissolved carbon species in associated diffuse and focused flow hydrothermal vents at the Main Endeavour Field, Juan de Fuca Ridge: phase equilibria and kinetic constraints. Geochem. Geophys. Geosys. 10.
Frank, M., Eckhardt, J.-D., Eisenhauer, A., Kubik, P.W., Dittrich-Hannen, B., Segl, M., Mangini, A., 1994. Beryllium 10, thorium 230, and protactinium 231 in Galapagos microplate sediments: Implications of hydrothermal activity and paleoproductivity changes during the last 100,000 years. Paleoceanography 9, 559–578.
Galbraith, E.D., Jaccard, S.L., 2015. Deglacial weakening of the oceanic soft tissue pump: global constraints from sedimentary nitrogen isotopes and oxygenation proxies. Quat. Sci. Rev. 109, 38–48.
Gartman, A., Luther, G.W., 2014. Oxidation of synthesized sub-micron pyrite (FeS2) in seawater. Geochim. Cosmochim. Acta 144, 96–108.
German, C.R., Seyfried Jr., W.E., 2014. 8.7 - hydrothermal processes. In: Holland, H.D., Turekian, K.K.B. (Eds.), Treatise on Geochemistry, 2nd edition. Elsevier, Oxford, pp. 191–233.
German, C.R., Klinkhammer, G.P., Edmond, J.M., Mitra, A., Elderfield, H., 1990. Hydrothermal scavenging of rare-earth elements in the oceans. Nature 345, 516–518.
Gieskes, J., Elderfield, H., R. Lawrence, J., Johnson, J., Meyers, B., Campbell, A., 1982. Geochemistry of interstitial waters and sediments, Leg 64, Gulf of California. Initial Reports DSDP, Leg 64, 1978–79.
Gillis, K.M., Coogan, L.A., 2019. A review of the geological constraints on the conductive boundary layer at the base of the hydrothermal system at mid-ocean ridges. Geochemistry, Geophys. Geosystems. https://doi.org/10.1029/2018GC007878.
Gillis, K.M., Muehlenbachs, K., Stewart, M., Gleeson, T., Karson, J., 2001. Fluid flow patterns in fast-spreading East Pacific Rise crust exposed at Hess Deep. J. Geophys. Res. 106, 26,311–26,329.
Gledhill, M., van den Berg, C.M.G., 1994. Determination of complexation of iron(III) with natural organic complexing ligands in seawater using cathodic stripping voltammetry. Mar. Chem. 47, 41–54.
Hardie, L.A., 1996. Secular variation in seawater chemistry: an explanation for the coupled secular variation in the mineralogies of marine limestones and potash evaporites over the past 600 m.y. Geology 24, 279–283.
Hay, W.W., Migdisov, A., Balukhovsky, A.N., Wold, C.N., Flogel, S., Soding, E., 2006. Evaporites and the salinity of the ocean during the Phanerozoic: implications for climate, ocean circulation and life. Palaeogeogr. Palaeoclimatol. Palaeoecol. 240, 3–46.
Haymon, R.M., 1983. Growth history of hydrothermal black smoker chimneys. Nature 301, 695–698.
Haymon, R.M., Kastner, M., 1986. Caminite: a new magnesium-hydroxide-sufate-hydrate mineral found in a submarine hydrothermal deposit, East Pacific Rise, 21°N. Am. Mineral. 71, 819–825.
Heft, K.L., Gillis, K.M., Pollack, H.N., Karson, J.A., Klein, E.M., 2008. Role of upwelling hydrothermal fluids in the development of alteration patterns at fast spreading ridges: evidence from the sheeted dike complex at Pito Deep. G-cubed. https://doi.org/10.1029/2007GC001926.
Herzberg, C., Condie, K., Korenaga, J., 2010. Thermal history of the Earth and its petrological expression. Earth Planet. Sci. Lett. 292, 79–88.
Ho, P., Lee, J.-M., Heller, M.I., Lam, P.J., Shiller, A.M., 2018. The distribution of dissolved and particulate Mo and V along the U.S. GEOTRACES East Pacific Zonal Transect (GP16): the roles of oxides and biogenic particles in their distributions in the oxygen deficient zone and the hydrothermal plume. Mar. Chem. 201, 242–255.
Humphris, S.E., Klein, F., 2018. Progress in deciphering the controls on the geochemistry of fluids in seafloor hydrothermal systems. Annu. Rev. Mar. Sci. 10, 315–343.
James, R.H., Rudnicki, M.D., Palmer, M.R., 1999. The alkali element and boron geochemistry of the Escanaba Trough sediment-hosted hydrothermal system. Earth Planet. Sci. Lett. 171, 157–169.
Kasting, J.F., Howard, M.T., Wallmann, K., Veizer, J., Shields, G., Jaffres, J., 2006. Paleoclimates, ocean depth, and the oxygen isotopic composition of seawater. Earth Planet. Sci. Lett. 252, 82–93.
Kelley, D.S., Karson, J.A., Fruh-Green, G.L., Yoerger, D.R., Shank, T.M., Butterfield, D.A., Hayes, J.M., Schrenk, M.O., Olson, E.J., Proskurowski, G., Jakuba, M., Bradley, A., Larson, B., Ludwig, K., Glickson, D., Buckman, K., Bradley, A.S., Brazelton, W.J., Roe, K., Elend, M.J., Delacour, A., Bernasconi, S.M., Lilley, M.D., Baross, J.A., Summons, R.T., Sylva, S.P., 2005. A serpentinite-hosted ecosystem: the lost city hydrothermal field. Science 307, 1428–1434.
Klein, E.M., Langmuir, C.H., 1987. Global correlation of ocean ridge basalt chemistry with axial depth and crustal thickness. Jour. Geophys. Res. 92, 8089–8115.
Kump, L.R., Seyfried, W.E., 2005. Hydrothermal Fe fluxes during the Precambrian: effect of low oceanic sulfate concentrations and low hydrostatic pressure on the composition of black smokers. Earth Planet. Sci. Lett. 235, 654–662.
Lemmon, E.W., McLinden, M.O., Friend, D.G., 2018. Thermophysical Properties of Fluid Systems. in NIST Chemistry WebBook, NIST Standard Reference Database Number 69, Eds. P.J. Linstrom and W.G. Mallard, National Institute of Standards and Technology, Gaithersburg MD, 20899, https://doi.org/10.18434/T4D303.
Lilley, M.D., Butterfield, D.A., Olson, E.J., Lupton, J.E., Macko, S.A., McDuff, R.E., 1993. Anomalous CH4 and NH4+ concentrations at an unsedimented mid-ocean-ridge hydrothermal system. Nature 364, 45–47.
Lilley, M.D., Feely, R.A., Trefry, J.H., 1995. Chemical and biological transformations in hydrothermal plumes. In: Humphris, S.E., Zierenberg, R.A., Millineaux, L.S., Thomson, R.E. (Eds.), Seafloor Hydrothermal Systems: Physical, Chemical, Biological, and Geological Interactions. Am. Geophys. Un, Washington, D.C., pp. 369–391.
Lilley, M.D., Butterfield, D.A., Lupton, J.E., Olson, E.J., 2003. Magmatic events can produce rapid changes in hydrothermal vent chemistry. Nature 422, 878–880.
Lister, C.R.B., 1995. Heat transfer between magmas and hydrothermal systems, or, six lemmas in search of a theorem. Geophys. J. Int. 120, 45–59.
Liu, X., Millero, F.J., 2002. The solubility of iron in seawater. Mar. Chem. 77, 43–54.
Lonsdale, P.F., Bischoff, J.L., Burns, V.M., Kastner, M., Sweeney, R.E., 1980. A high-temperature hydrothermal deposit on the seabed at a gulf of California spreading center. Earth Planet. Sci. Lett. 49, 8–20.
Lowell, R.P., Yao, Y., Germanovich, L.N., 2003. Anhydrite precipitation and the relationship between focused and diffuse flow in seafloor hydrothermal systems. J. Geophys. Res. 108 (B9), 2424. https://doi.org/10.1029/2002JB002371.
Lowell, R.P., Farough, A., Hoover, J., Cummings, K., 2013. Characteristics of magma-driven hydrothermal systems at oceanic spreading centers. Geochem. Geophys. Geosys. 14, 1756–1770.
Lowenstein, T.K., Hardie, L.A., Timofeeff, M.N., Demicco, R.V., 2003. Secular variation in seawater chemistry and the origin of calcium chloride basinal brines. Geology 31, 857–860.
Lowenstein, T.K., Kendall, B., Anbar, A.D., 2014. The geologic history of seawater. In: Treastise on Geochemistry, 2nd edition. vol. Volume 8. pp. 569–621.
Lund, D.C., Asimow, P.D., 2011. Does sea level influence mid-ocean ridge magmatism on Milankovitch timescales? Geochemistry, Geophys. Geosystems 12 (n/a–n/a).
Lund, D.C., Asimow, P.D., Farley, K.A., Rooney, T.O., Seeley, E., Jackson, E.W., Durham, Z.M., 2016. Enhanced East Pacific Rise hydrothermal activity during the last two glacial terminations. Science 351, 478–482.
Lupton, J.E., Craig, H., 1981. A major helium-3 source at 15°S on the East Pacific Rise. Science 214, 13 LP–18.
Mangini, A., Eisenhauer, A., Walter, P., 1990. Response of manganese in the ocean to the climatic cycles in the Quaternary. Paleoceanography 5, 811–821.
Martens, C.S., 1990. Generation of short chain acid anions in hydrothermally altered sediments of the Guaymas Basin, Gulf of California. Appl. Geochem. 5, 71–76.
McDermott, J.M., Sylva, S.P., Ono, S., German, C.R., Seewald, J.S., 2018. Geochemistry of fluids from Earth's deepest ridge-crest hot-springs: piccard hydrothermal field, Mid-Cayman Rise. Geochim. Cosmochim. Acta 228, 95–118.
Metz, S., Trefry, J.H., 1993. Field and laboratory studies of metal uptake and release by hydrothermal precipitates. J. Geophys. Res. Solid Earth 98, 9661–9666.
Middleton, J.L., Langmuir, C.H., Mukhopadhyay, S., McManus, J.F., Mitrovica, J.X., 2016. Hydrothermal iron flux variability following rapid sea level changes. Geophys. Res. Lett. 43, 3848–3856.
Miller, K.G., Kominz, M.A., Browning, J.V., Wright, J.D., Mountain, G.S., Katz, M.E., Sugarman, P.J., Cramer, B.S., Christie-Blick, N., Pekar, S.F., 2005. The Phanerozoic record of global sea-level change. Science 310, 1293–1298.
Millero, F.J., Sotolongo, S., Izaguirre, M., 1987. The oxidation kinetics of Fe(II) in

seawater. Geochim. Cosmochim. Acta 51, 793–801.
Mills, R.A., Taylor, S.L., Pälike, H., Thomson, J., 2010. Hydrothermal sediments record changes in deep water oxygen content in the SE Pacific. Paleoceanography 25. https://doi.org/10.1029/2010PA001959.
Mottl, M.J., Holland, H.D., 1978. Chemical exchange during hydrothermal alteration of basalt by seawater—I. Experimental results for major and minor components of seawater. Geochim. Cosmochim. Acta 42, 1103–1115.
Mottl, M.J., McConachy, T.F., 1990. Chemical processes in buoyant hydrothermal plumes on the East Pacific Rise near 21°N. Geochim. Cosmochim. Acta 54, 1911–1927.
Mottl, M.J., Holland, H.D., Corr, R.F., 1979. Chemical exchange during hydrothermal alteration of basalt by seawater—II. Experimental results for Fe, Mn, and sulfur species. Geochim. Cosmochim. Acta 43, 869–884.
Müller, R.D., Sdrolias, M., Gaina, C., Steinberger, B., Heine, C., 2008. Long-term sea-level fluctuations driven by ocean basin dynamics. Science 319, 1357–1362.
Müller, R.D., Dutkiewicz, A., Seton, M., Gaina, C., 2013. Seawater chemistry driven by supercontinent assembly, breakup, and dispersal. Geology 41, 907–910.
Norton, D.L., 1984. Theory of hydrothermal systems. Annu. Rev. Earth Planet. Sci. 12, 155–177.
Ono, S., Shanks, W.C., Rouxel, O.J., Rumble, D., 2007. S-33 constraints on the seawater sulfate contribution in modern seafloor hydrothermal vent sulfides. Geochim. Cosmochim. Acta 71, 1170–1182.
Palliser, C., McKibbin, R., 1998. A model for deep geothermal brines III: thermodynamic properties - enthalpy and viscosity. Transp. Porous Media 33, 155–171.
Pavia, F., Anderson, R., Vivancos, S., Fleisher, M., Lam, P., Lu, Y., Cheng, H., Zhang, P., Edwards, R.L., 2018. Intense hydrothermal scavenging of ^{230}Th and ^{231}Pa in the deep Southeast Pacific. Mar. Chem. 201, 212–228.
Pester, N.J., 2018. Effects of Sea Level Change on the Deep-Sea Hydrothermal Flux of Transition Metals to the Ocean. Goldschmidt Abstracts, Boston, MA, USA (12-17 Aug).
Pester, N.J., Butterfield, D.A., Foustoukos, D.I., Roe, K.K., Ding, K., Shank, T.M., Seyfried, W.E., Jr., 2008. The chemistry of diffuse-flow vent fluids on the Galapagos Rift (86°W): temporal variability and subseafloor phase equilibria controls, in: Lowell, R. P., Seewald, J.S., Perfit, M.R., Metaxas, A. (Eds.), Magma to Microbe: Modeling Hydrothermal Processes at Oceanic Spreading Centers, Geophys. Monogr. Ser., vol. 178. AGU, Washington, D.C., pp. 123–144.
Pester, N.J., Rough, M., Ding, K., Seyfried Jr., W.E., 2011. A new Fe/Mn geothermometer for hydrothermal systems: implications for high-salinity fluids at 13°N on the East Pacific Rise. Geochim. Cosmochim. Acta 75, 7881–7892.
Pester, N.J., Reeves, E.P., Rough, M.E., Ding, K., Seewald, J.S., Seyfried, W.E., Jr., 2012. Subseafloor phase equilibria in high-temperature hydrothermal fluids of the Lucky Strike Seamount (Mid-Atlantic Ridge, 37°17'N). Geochim. Cosmochim. Acta 90, 303–322.
Pester, N., Ding, K., E Seyfried, W., 2014. Magmatic eruptions and iron volatility in deep-sea hydrothermal fluids. Geology 42, 255.
Pester, N.J., Ding, K., Seyfried, W.E., 2015. Vapor–liquid partitioning of alkaline earth and transition metals in NaCl-dominated hydrothermal fluids: an experimental study from 360 to 465°C, near-critical to halite saturated conditions. Geochim. Cosmochim. Acta 168, 111–132.
Pokrovski, G.S., Roux, J., Harrichoury, J.-C., 2005. Fluid density control on vapor-liquid partitioning of metals in hydrothermal systems. Geol 33, 657–660.
Pokrovski, G.S., Borisova, A.Y., Harrichoury, J.-C., 2008. The effect of sulfur on vapor–liquid fractionation of metals in hydrothermal systems. Earth Planet. Sci. Lett. 266, 345–362.
Rae, J.W.B., Sarnthein, M., Foster, G.L., Ridgwell, A., Grootes, P.M., Elliott, T., 2014. Deep water formation in the North Pacific and deglacial CO_2 rise. Paleoceanography 29, 645–667.
Ramondenc, P., Germanovich, L.N., Von Damm, K.L., Lowell, R.P., 2006. The first measurements of hydrothermal heat output at 9°50'N, East Pacific Rise. Earth Planet. Sci. Lett. 245, 487–497.
Ravizza, G., Blusztajn, J., Von Damm, K.L., Bray, A.M., Bach, W., Hart, S.R., 2001. Sr isotopes variations in vent fluids from 9°46′-9°45'N East Pacific Rise: evidence of a non-zero-Mg fluid component. Geochim. Cosmochim. Acta 65, 729–739.
Reid, I., Jackson, H.R., 1981. Oceanic spreading rate and crustal thickness. Mar. Geophys. Res. 5, 165–172.
Resing, J.A., Sedwick, P.N., German, C.R., Jenkins, W.J., Moffett, J.W., Sohst, B.M., Tagliabue, A., 2015. Basin-scale transport of hydrothermal dissolved metals across the South Pacific Ocean. Nature 523, 200.
Roshan, S., Wu, J., Jenkins, W.J., 2016. Long-range transport of hydrothermal dissolved Zn in the tropical South Pacific. Mar. Chem. 183, 25–32.
Rouxel, O., Shanks, W.C., Bach, W., Edwards, K.J., 2008. Integrated Fe- and S-isotope study of seafloor hydrothermal vents at East Pacific rise 9-10 degrees N. Chem. Geol. 252, 214–227.
Rudnicki, M.D., Elderfield, H., 1993. A chemical model of the buoyant and neutrally buoyant plume above the TAG vent field, 26 degrees N, Mid-Atlantic Ridge. Geochim. Cosmochim. Acta 57, 2939–2957.
Ruhlin, D.E., Owen, R.M., 1986. The rare earth element geochemistry of hydrothermal sediments from the East Pacific Rise: examination of a seawater scavenging mechanism. Geochim. Cosmochim. Acta 50, 393–400.
Saccocia, P.J., Seyfried, W.E., 1994. The solubility of chlorite solid-solutions in 3.2 wt-percent NaCl fluids from 300-400-degrees-C, 500 bars. Geochim. Cosmochim. Acta 58, 567–585.
Schaller, T., Morford, J., Emerson, S.R., Feely, R.A., 2000. Oxyanions in metalliferous sediments: tracers for paleoseawater metal concentrations? Geochim. Cosmochim. Acta 64, 2243–2254.
Scheuermann, P.P., Tan, C., Seyfried Jr., W.E., 2018. Quartz solubility in the two-phase region of the NaCl-H2O system: an experimental study with application to the Piccard hydrothermal field, Mid-Cayman Rise. Geochem. Geophys. Geosyst. 19, 3570–3582.
Schoofs, S., Hansen, U., 2000. Depletion of a brine layer at the base of ridge-crest hydrothermal systems. Earth Planet. Sci. Lett. 180, 341–353.
Schultz, A., Delaney, J.R., McDuff, R.E., 1992. On the partitioning of heat flux between diffuse and point source seafloor venting. Jour. Geophys. Res. 97, 12,212–299,314.
Seyfried, W.E., Ding, K., 1995. Phase equilibria in subseafloor hydrothermal systems: a review of the role of redox, temperature, pH, and dissolved Cl on the chemistry of hot spring fluids at mid-ocean ridges. In: Humphris, S.E., Zierenberg, R.A., Millineaux, L.S., Thomson, R.E. (Eds.), Seafloor Hydrothermal Systems: Physical, Chemical, Biological, and Geological Interactions. Am. Geophys. Un, Washington, D.C., pp. 248–272.
Seyfried Jr., W.E., 1987. Experimental and theoretical constraints on hydrothermal alteration processes at mid-ocean ridges. Annu. Rev. Earth Planet. Sci. 15, 317–335.
Seyfried Jr., W.E., Bischoff, J.L., 1981. Experimental seawater-basalt interaction at 300°C, 500 bars, chemical exchange, secondary mineral formation and implications for the transport of heavy metals. Geochim. Cosmochim. Acta 45, 135–147.
Seyfried Jr., W.E., Ding, K., Berndt, M.E., 1991. Phase equilibria constraints on the chemistry of hot spring fluids at mid-ocean ridges. Geochim. Cosmochim. Acta 55, 3559–3580.
Seyfried, W.E., Ding, K., Rao, B., 2002. Experimental calibration of metastable plagioclase-epidote-fluid equilibria at elevated temperatures and pressures: applications to the chemistry of hydrothermal fluids at mid-ocean ridges. In: Hellmann, R., Wood, S.A. (Eds.), Water-Rock Interactions, Ore Deposits, and Environmental Geochemistry: A Tribute to David a. Crerar, pp. 257–278.
Seyfried, W.E., Seewald, J.S., Berndt, M.E., Ding, K., Foustoukos, D.I., 2003. Chemistry of hydrothermal vent fluids from the Main Endeavour Field, northern Juan de Fuca Ridge: geochemical controls in the aftermath of June 1999 seismic events. J. Geophys. Res. Earth 108. https://doi.org/10.1029/2002JB001957.
Seyfried, W.E., Pester, N.J., Ding, K., Rough, M., 2011. Vent fluid chemistry of the Rainbow hydrothermal system (36°N, MAR): phase equilibria and in situ pH controls on subseafloor alteration processes. Geochim. Cosmochim. Acta 75, 1574–1593.
Shanks, W.C., 2001. Stable isotopes in seafloor hydrothermal systems. In: Valley, J.W., Cole, D.R. (Eds.), Stable Isotope Geochemistry. Mineralogical Society of America, pp. 469–526.
Simoneit, B.R.T., Goodfellow, W.D., Franklin, J.M., 1992. Hydrothermal petroleum at the seafloor and organic matter alteration in sediments of Middle Valley, Northern Juan de Fuca Ridge. Appl. Geochem. 7, 257–264.
Sleep, N.H., 1991. Hydrothermal circulation, anhydrite precipitation, and thermal structure at ridge axes. J. Geophys. Res. 96, 2375–2387.
Speer, K.G., Rona, P.A., 1989. A model of an Atlantic and Pacific hydrothermal plume. J. Geophys. Res. Ocean. 94, 6213–6220.
Spivack, A.J., Edmond, J.M., 1987. Boron isotope exchange between seawater and the oceanic crust. Geochim. Cosmochim. Acta 51, 1033–1043.
Tagliabue, A., Bopp, L., Dutay, J.C., Bowie, A.R., Chever, F., Jean-Baptiste, P., Bucciarelli, E., Lannuzel, D., Remenyi, T., Sarthou, G., Aumont, O., Gehlen, M., Jeandel, C., 2010. Hydrothermal contribution to the oceanic dissolved iron inventory. Nat. Geosci. 3, 252–256.
Teske, A., Hinrichs, K.-U., Edgcomb, V., de Vera Gomez, A., Kysela, D., Sylva, S.P., Sogin, M.L., Jannasch, H.W., 2002. Microbial diversity of hydrothermal sediments in the Guaymas Basin: evidence for anaerobic methanotrophic communities. Appl. Environ. Microbiol. 68, 1994 LP–2007.
Tivey, M.K., 2007. Generation of seafloor hydrothermal vent fluids and associated mineral deposits. Oceanography 20, 50–65.
Turchyn, A.V, Alt, J.C., Brown, S.T., DePaolo, D.J., Coggon, R.M., Chi, G., Bédard, J.H., Skulski, T., 2013. Reconstructing the oxygen isotope composition of late Cambrian and Cretaceous hydrothermal vent fluid. Geochim. Cosmochim. Acta 123, 440–458.
Von Damm, K.L., 1995. Controls on the chemistry and temporal variability of seafloor hydrothermal fluids. In: Humphris, S.E., Zierenberg, R.A., Millineaux, L.S., Thomson, R.E. (Eds.), Seafloor Hydrothermal Systems: Physical, Chemical, Biological, and Geological Interactions. Am. Geophys. Un, Washington, D.C., pp. 222–247.
Von Damm, K.L., 2000. Chemistry of hydrothermal vent fluids from 9°-10°N, East Pacific Rise: "Time zero" the intermediate post-eruptive period. Jour. Geophys. Res. 105, 11,203–211,222.
Von Damm, K.L., Edmond, J.M., Grant, B., Measures, C.I., Walden, B., Weiss, R.F., 1985a. Chemistry of submarine hydrothermal solutions at 21°N, East Pacific Rise. Geochim. Cosmochim. Acta 49, 2197–2220.
Von Damm, K.L., Edmond, J.M., Measures, C.I., Grant, B., 1985b. Chemistry of submarine hydrothermal solutions at Guaymas Basin, Gulf of California. Geochim. Cosmochim. Acta 49, 2221–2237.
Von Damm, K.L., Lilley, M.D., Shanks, W.C., Brockington, M., Bray, A.M., O'Grady, K.M., Olson, E., Graham, A., Proskurowski, G., 2003. Extraordinary phase separation and segregation in vent fluids from the southern East Pacific Rise. Earth Planet. Sci. Lett. 206, 365–378.
Wetzel, L.R., Shock, E.L., 2000. Distinguishing ultramafic-from basalt-hosted submarine hydrothermal systems by comparing calculated vent fluid compositions. J. Geophys. Res. Solid Earth 105, 8319–8340.
Yu, J., Anderson, R.F., Jin, Z., Rae, J.W.B., Opdyke, B.N., Eggins, S.M., 2013. Responses of the deep ocean carbonate system to carbon reorganization during the Last Glacial–interglacial cycle. Quat. Sci. Rev. 76, 39–52.